

# Probing Bose-enhanced Inflaton Decay with Gravitational Waves

---

Nicolás Bernal  <sup>a</sup> Quan-feng Wu  <sup>b,c</sup> Xun-Jie Xu  <sup>b</sup> and Yong Xu  <sup>d</sup>

<sup>a</sup> *New York University Abu Dhabi*

*PO Box 129188, Saadiyat Island, Abu Dhabi, United Arab Emirates*

<sup>b</sup> *Institute of High Energy Physics, Chinese Academy of Sciences, Beijing 100049, China*

<sup>c</sup> *Kaiping Neutrino Research Center, Kaiping 529386, China*

<sup>d</sup> *McGill University Department of Physics & Trottier Space Institute  
3600 Rue University, Montréal, QC, H3A 2T8, Canada*

*E-mail:* [nicolas.bernal@nyu.edu](mailto:nicolas.bernal@nyu.edu), [wuquanfeng@ihep.ac.cn](mailto:wuquanfeng@ihep.ac.cn),  
[xuxj@ihep.ac.cn](mailto:xuxj@ihep.ac.cn), [yong.xu6@mcgill.ca](mailto:yong.xu6@mcgill.ca)

**ABSTRACT:** We investigate cosmic reheating dynamics in the presence of a transient condensate formed by bosonic decay products of the inflaton. We show that the emergence of such a condensate and the corresponding Bose enhancement can dramatically increase the efficiency of inflaton decay, giving rise to qualitatively new reheating dynamics beyond the standard perturbative picture. As a consequence, graviton production from inflaton decay processes is significantly amplified by Bose enhancement effects, leading to a stochastic gravitational-wave background with a potentially observable amplitude, even in the low-frequency regime.

---

## Contents

<b>1</b>	<b>Introduction</b>	<b>1</b>
<b>2</b>	<b>Reheating through inflaton decay</b>	<b>2</b>
2.1	Inflaton decay without Bose enhancement	2
2.2	Inflaton decay with Bose enhancement	5
<b>3</b>	<b>Production of gravitational waves</b>	<b>9</b>
3.1	General formalism	9
3.2	$\varphi\varphi \rightarrow hh$	11
3.3	$\phi \rightarrow \varphi\varphi h$	13
3.3.1	$\phi \rightarrow \varphi_B \varphi_B h$	13
3.3.2	$\phi \rightarrow \varphi_B \varphi h$	15
3.3.3	$\phi \rightarrow \varphi \varphi h$	15
3.4	$\varphi\phi \rightarrow \varphi h$	16
3.5	$\phi\phi \rightarrow hh$	16
<b>4</b>	<b>Conclusions</b>	<b>17</b>
<b>A</b>	<b>Phase space integrals for the 1-to-2 process</b>	<b>18</b>
<b>B</b>	<b>Solving the Boltzmann equation of <math>f_\varphi</math></b>	<b>21</b>
<b>C</b>	<b>Phase space integrals for graviton production processes</b>	<b>22</b>

---

## 1 Introduction

Gravitons are unique messengers from the very early Universe: once produced, they propagate essentially freely and retain detailed information about the cosmological background at their origin. Consequently, the spectrum of a stochastic gravitational-wave (GW) background provides a powerful and direct probe of primordial dynamics.

In inflationary cosmology, gravitons can be abundantly produced during the cosmic reheating epoch after inflation, when inflatons transfer their energy to the visible sector; for reviews of reheating, see, e.g., [1–4]. Even in the minimal realization of reheating via perturbative inflaton decay, graviton production is unavoidable due to the universal coupling of gravity to energy–momentum of the matter content. Various processes contribute during this stage, including graviton bremsstrahlung from inflaton decay [5–18], inflaton pair annihilation [19–23], scattering between the inflaton and its decay products [24–26], and purely scattering processes among the daughter particles [26, 27].

However, a generic challenge arises from the Planck suppression of gravitational interactions. Achieving a sizable GW amplitude typically requires a high characteristic energy scale, pushing the peak of the GW spectrum into the ultra-high-frequency regime and favoring large inflaton masses and/or high reheating temperatures. This substantially limits the detectability of GWs generated during reheating, given the current lack of sufficiently sensitive high-frequency detectors [28, 29].

Recently, we demonstrated that this limitation can be overcome if the inflaton scatters with a non-thermalized bosonic decay product, dubbed the *reheaton* [25]. During the pre-thermalization stage, the reheaton occupation number can become parametrically large, enhancing graviton production and allowing for an observable GW signal even for comparatively small inflaton masses. This enhancement simultaneously shifts the GW spectrum toward lower frequencies, improving the detection prospects.

In this work, we uncover a qualitatively new and even more powerful realization of this idea with transient *reheaton condensation*. We show that when the reheaton forms a condensate, quantum-statistical enhancement dramatically alters the inflaton decay dynamics and opens entirely new, highly efficient channels for graviton production. This mechanism leads to GW signals with amplitudes and spectral features that are markedly distinct from those of previously studied reheating scenarios, providing a novel observational window into the microscopic physics of reheating.

The remainder of this work is organized as follows. In Section 2, we present the formalism of inflaton decay, with particular emphasis on Bose enhancement effects. The resulting GW spectra are discussed in Section 3. Our main conclusions are summarized in Section 4. Technical details of the phase-space integrations and computations for collision terms are relegated to the Appendices.

## 2 Reheating through inflaton decay

In this section, the cosmic reheating era is studied in the context of a perturbative decay of the inflaton field.<sup>1</sup> Inflatons decay into pairs of light mediator particles (the reheatons), which are assumed to have no sizable self-interactions, such that they only redshift without reaching kinetic or chemical equilibrium. We first review the standard scenario where the decay proceeds without Bose enhancement, followed by the case of a Bose-enhanced inflaton decay. Eventually, at late times, all reheatons transfer their energy to SM particles, while still being relativistic.

### 2.1 Inflaton decay without Bose enhancement

Let us start with one of the simplest perturbative reheating scenarios: inflaton decay. After inflation, the inflaton field  $\phi$  oscillates at the bottom of its potential, which we assume to be quadratic. This leads to a matter-dominated epoch during which the Universe is filled with cold  $\phi$  particles. If  $\phi$  is assumed to have a small perturbative decay width,  $\phi \rightarrow \varphi\varphi$ , where  $\varphi$  is a light relativistic boson called the reheaton throughout this work, all  $\phi$  particles

---

<sup>1</sup>This simplified setup is adopted to illustrate the underlying physical mechanism. For non-perturbative reheating scenarios, including preheating, we refer the reader to the reviews in Refs. [1–4].

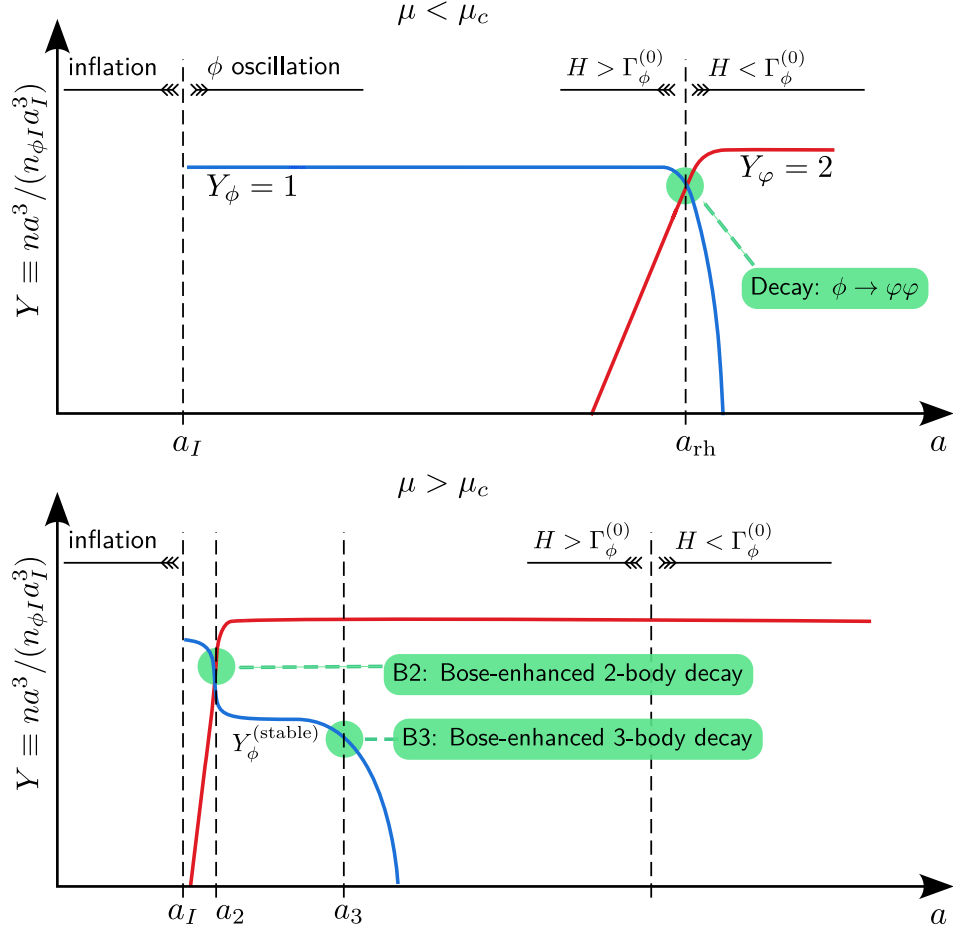


**Figure 1.** Schematic illustration of the evolution of the normalized comoving number densities  $Y$  of inflatons ( $\phi$ , blue lines) and reheatons ( $\varphi$ , red lines) with (bottom panel,  $\mu \gg \mu_c$ ) and without (top panel,  $\mu \ll \mu_c$ ) Bose enhancement, as a function of the cosmic scale factor  $a$ .

will gradually decay, releasing their energy to  $\varphi$ , resulting in a radiation-dominated era. This is illustrated in the upper panel of Fig. 1, where the blue and red lines represent the normalized comoving number densities  $Y$  of  $\phi$  and  $\varphi$ , respectively.

Quantitatively, it is possible to calculate this reheating process, starting from the relevant Lagrangian density

$$\mathcal{L} \supset -\frac{1}{2} m_\phi^2 \phi^2 - \frac{\mu}{2} \phi \varphi^2, \quad (2.1)$$

where  $m_\phi$  denotes the mass of the inflaton and  $\mu$  is a dimension-one coupling. Here, the bare mass term for the reheaton is ignored, as it is assumed to be always relativistic. In addition, as we focus on a non-thermal reheaton, possible trilinear and quartic self-interactions are assumed to be subdominant. For later convenience, we also define the dimensionless coupling

$$y \equiv \frac{\mu}{m_\phi}. \quad (2.2)$$

From the Feynman diagrammatic perspective, the theory is perturbative as long as  $y^2 \ll$

$4\pi$ . The tree-level decay rate of  $\phi \rightarrow \varphi\varphi$  reads

$$\Gamma_\phi^{(0)} \simeq \frac{\mu^2}{32\pi m_\phi} = \frac{y^2}{32\pi} m_\phi. \quad (2.3)$$

Note that  $\Gamma_\phi^{(0)}$  corresponds to the *in-vacuum* decay rate. In the early Universe with a dense background of particles, the actual decay rate, denoted by  $\Gamma_\phi$ , may be significantly different from  $\Gamma_\phi^{(0)}$  in Eq. (2.3). Nevertheless, if the decay occurs sufficiently slow (that is, for  $\mu$  sufficiently small), the difference can be safely ignored, and Eq. (2.3) can be used. This statement will be quantified in the next section.

The number densities of  $\phi$  and  $\varphi$ , denoted by  $n_\phi$  and  $n_\varphi$ , are governed by the following set of Boltzmann equations

$$\frac{dn_\phi}{dt} + 3H n_\phi = -\Gamma_\phi n_\phi, \quad (2.4)$$

$$\frac{dn_\varphi}{dt} + 3H n_\varphi = +2\Gamma_\phi n_\phi, \quad (2.5)$$

where  $H \equiv \dot{a}/a$  is the Hubble expansion rate with  $a$  the cosmic scale factor. It is determined by

$$H^2 = \frac{\rho_\phi + \rho_\varphi}{3M_P^2}, \quad (2.6)$$

where  $\rho_{\phi,\varphi}$  denotes the energy density of  $\phi$  and  $\varphi$ , and  $M_P \equiv 1/\sqrt{8\pi G_N} \simeq 2.435 \times 10^{18}$  GeV, with  $G_N$  being Newton's gravitational constant, is the reduced Planck mass. In Eq. (2.5), we assume that  $\varphi$  is produced only through  $\phi \rightarrow \varphi\varphi$ , while other processes that could potentially change the number of  $\varphi$  particles (e.g.  $\varphi \rightarrow \text{SM}$ ,  $\phi \rightarrow 4\varphi$ ,  $2\varphi \rightarrow 4\varphi$ ) are highly suppressed.

Taking  $\Gamma_\phi = \Gamma_\phi^{(0)}$ , Eqs. (2.4) and (2.5) can be analytically solved from the beginning of reheating at  $a = a_I$ . Taking  $n_\phi(a_I) \equiv n_{\phi I} = 3H_I^2 M_P^2 / m_\phi$  and  $n_\varphi(a_I) = 0$  as initial conditions, one gets [25]

$$n_\phi(a) = n_{\phi I} \left( \frac{a_I}{a} \right)^3 \exp \left[ -\Gamma_\phi^{(0)} t \right], \quad (2.7)$$

$$n_\varphi(a) = 2 \left[ n_{\phi I} \left( \frac{a_I}{a} \right)^3 - n_\phi(a) \right], \quad (2.8)$$

with

$$t \simeq \frac{2}{3H_I} \left[ \left( \frac{a}{a_I} \right)^{3/2} - 1 \right]. \quad (2.9)$$

The evolution of the normalized comoving number densities

$$Y_i(a) \equiv \frac{n_i}{n_{\phi I}} \left( \frac{a}{a_I} \right)^3 \quad (2.10)$$

with  $i = \phi$  and  $\varphi$  is schematically illustrated in the upper panel of Fig. 1.

Before ending this section, we note that the trilinear inflaton–reheaton coupling  $\mu$  in Eq. (2.1) can induce an effective mass term for the latter, proportional to the inflaton

field value  $\phi$ , thus modifying the decay kinematics [30–32]. To properly account for this effect, one should average over the inflaton oscillations, which leads to an effective coupling  $\mu_{\text{eff}}$  for the interaction in Eq. (2.3). For the quadratic inflaton potential considered here, this effect has been shown to be moderate, yielding  $\mu_{\text{eff}} \simeq \mu$  [30, 32]. Moreover, this coupling could also lead to a tachyonic mass for the daughter field when the inflaton crosses zero during its oscillations, potentially triggering nonperturbative particle production via tachyonic resonance [33]. However, even a small self-interaction of the daughter field, such as a  $\lambda \varphi^4$  term, generates a positive effective mass-squared contribution of order  $\lambda \langle \varphi^2 \rangle$ , which counteracts the tachyonic instability. Here,  $\langle \varphi^2 \rangle$  denotes the field variance, i.e., the expectation value of the squared reheaton field, which grows as particles are produced and provides a dynamical mass that stabilizes the system. As a result, nonperturbative energy transfer becomes subdominant due to backreaction, and the inflaton energy is primarily transferred via perturbative decay. In this work, we restrict our analysis to the simplest perturbative scenario and illustrate the effectiveness of Bose enhancement in draining the inflaton energy even in the perturbative regime.

## 2.2 Inflaton decay with Bose enhancement

The treatment in Section 2.1 is valid as long as the decay of  $\phi$  is not affected by the cosmological background. However, if  $\phi$  decays fast, the number density of the decay product,  $\varphi$ , can increase rapidly to a level at which its influence on the decay can no longer be ignored.

Qualitatively, one can anticipate that the decay is enhanced by the presence of the  $\varphi$  background due to its *bosonic* nature. As  $\mu$  increases, the Bose enhancement effect is enhanced due to the rapidly-created  $\varphi$  background. Quantitatively, this can be calculated from the following unintegrated Boltzmann equation

$$\left( \frac{\partial}{\partial t} - H p \frac{\partial}{\partial p} \right) f(t, p) = \mathcal{C}[f], \quad (2.11)$$

where  $f(t, p)$  is the phase-space distribution function of the species under consideration and  $\mathcal{C}[f]$  is the collision term. The most general form of  $\mathcal{C}[f]$  is well known and can be found in cosmology textbooks (e.g., see Ref. [34]). After performing the phase space integration in  $\mathcal{C}[f]$  (see Appendix A for the detailed derivation), we obtain

$$\mathcal{C}[f_\phi] = -\Gamma_\phi^{(0)} f_\phi \mathcal{B}_e, \quad (2.12)$$

$$\mathcal{C}[f_\varphi] = +\frac{16\pi^2 \Gamma_\phi^{(0)} n_\phi}{m_\phi^2} \delta\left(p_\varphi - \frac{m_\phi}{2}\right) \mathcal{B}_e, \quad (2.13)$$

where the Bose-enhancement factor  $\mathcal{B}_e$  is given by

$$\mathcal{B}_e \equiv 1 + f_\varphi\left(t, \frac{m_\phi}{2}\right). \quad (2.14)$$

If we further integrate out the phase space of  $\phi$  or  $\varphi$ , Eqs. (2.12) and (2.13) lead to

$$\int \mathcal{C}[f_\phi] \frac{4\pi p_\phi^2 dp_\phi}{(2\pi)^3} = -n_\phi \Gamma_\phi^{(0)} \mathcal{B}_e, \quad (2.15)$$

$$\int \mathcal{C}[f_\varphi] \frac{4\pi p_\varphi^2 dp_\varphi}{(2\pi)^3} = +2 n_\phi \Gamma_\phi^{(0)} \mathcal{B}_e. \quad (2.16)$$

This should be compared with the right-hand sides of Eqs. (2.4) and (2.5), implying

$$\Gamma_\phi = \Gamma_\phi^{(0)} \mathcal{B}_e. \quad (2.17)$$

Obviously, in the absence of Bose enhancement,  $\mathcal{B}_e \rightarrow 1$ ,  $\Gamma_\phi$  becomes identical to  $\Gamma_\phi^{(0)}$ , while  $\mathcal{C}[f_\phi]$  and  $\mathcal{C}[f_\varphi]$  recover their respective forms in the case of Maxwell-Boltzmann statistics.

A highly non-trivial feature of the above formalism including Bose enhancement is the following series of consequences:

$\text{increasing } f_\varphi \rightarrow \text{increasing } \mathcal{B}_e \rightarrow \text{enhanced decay rate} \rightarrow \text{increasing } f_\varphi.$

The first and second steps can be immediately seen from Eqs. (2.14) and (2.17). The last step is valid until the remaining  $\phi$  particles are insufficient to support Bose-enhanced decay. Due to this closed positive-feedback loop, the system exhibits strongly nonlinear behavior. Under certain conditions, the feedback loop can lead to instability, causing  $\phi$  to decay at an extremely rapid rate.

In the following, we study this nonlinear behavior analytically. Substituting Eq. (2.13) into Eq. (2.11) and assuming that the evolution of  $n_\phi$  is known, one can solve the Boltzmann equation analytically (see Appendix B) and obtain

$$f_\varphi = \exp \left[ \frac{\pi \mu^2}{m_\phi^4} \frac{n_\phi(a x_\varphi)}{H(a x_\varphi)} \Theta \left[ \frac{a_I}{a} \leq x_\varphi \leq 1 \right] \right] - 1, \quad (2.18)$$

where

$$x_\varphi \equiv \frac{2 p_\varphi}{m_\phi}. \quad (2.19)$$

Substituting Eq. (2.18) into Eq. (2.14), we obtain

$$\mathcal{B}_e = \exp \left[ \frac{\pi \mu^2}{m_\phi^4} \frac{n_\phi(a)}{H(a)} \right]. \quad (2.20)$$

It is convenient to rewrite Eq. (2.4) as

$$\frac{1}{a^3} \frac{d(n_\phi a^3)}{da} = -\frac{\Gamma_\phi^{(0)}}{a H} \mathcal{B}_e n_\phi, \quad (2.21)$$

which is equivalent to

$$\frac{dY_\phi}{da} = -\beta Y_\phi, \quad (2.22)$$

where

$$\beta \equiv \frac{\Gamma_\phi^{(0)}}{a H} \exp \left[ \frac{\pi \mu^2 n_{\phi I}}{m_\phi^4 H} \left( \frac{a_I}{a} \right)^3 Y_\phi \right], \quad (2.23)$$

with  $\beta$  being the depletion rate of  $Y_\phi$ . The exponential dependence on the trilinear coupling  $\mu$  in  $\beta$  has an important implication: if the exponent exceeds a critical value, inflatons decay almost instantaneously, exponentially fast.

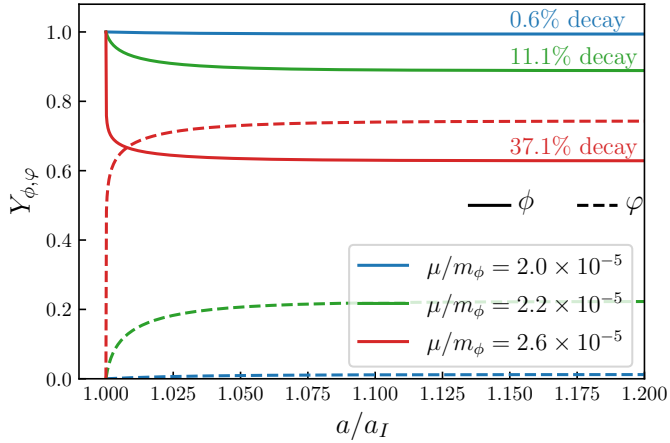


**Figure 2.** Numerical examples showing how the evolution of the normalized comoving number densities for  $\phi$  and  $\varphi$  are strongly affected by small variations of  $\mu$  around the critical value  $\mu_c$ . It is assumed  $m_\phi = 10^{13}$  GeV and  $H_I/m_\phi = 0.1$ .

To illustrate this exponential sensitivity, we inspect several numerical examples. For  $m_\phi = 10^{13}$  GeV,  $H_I/m_\phi = 0.1$  and  $\mu/m_\phi = \{2, 3, 4\} \times 10^{-5}$ , the corresponding values of  $\Gamma_\phi^{(0)}$  and  $\beta$  are  $\Gamma_\phi^{(0)} \simeq \{4, 9, 16\} \times 10^{-12} m_\phi \ll H_I$  and  $\beta \simeq \{0.2, 6 \times 10^{11}, 10^{29}\}$ . The last two cases indicate that  $Y_\phi$  should decrease almost instantly. To further inspect how the evolution of  $Y_\phi$  is affected by the Bose enhancement, we present numerical solutions of Eq. (2.22) with  $\mu/m_\phi = \{2.0, 2.2, 2.6\} \times 10^{-5}$  in Fig. 2. The case  $\mu/m_\phi = 2 \times 10^{-5}$  leads to a very insignificant decay (only 0.6%) of inflatons. When  $\mu/m_\phi$  increases to  $2.2 \times 10^{-5}$ , a significant portion (11.1%) of the inflatons decay rapidly due to the Bose enhancement. The decrease in  $Y_\phi$  by 11.1% simply reflects the increase in  $\sim 10\%$  of  $\mu$ . However, increasing further  $\mu/m_\phi$  to  $2.6 \times 10^{-5}$  translates into a rapid decay of more than a third of the inflatons, producing a large number of reheatons with  $n_\varphi > n_\phi$ . We emphasize that this behavior corresponds to the first depletion of inflatons shown in the lower panel of Fig. 1, and that eventually, at later times, all remaining inflatons will decay.

Since the condition required for rapid depletion of  $Y_\phi$  is  $\beta \gg 1$ , one can use it to derive the critical value of  $\mu$  for this to occur, together with the final stable value of  $Y_\phi$  after depletion. As  $Y_\phi$  decreases, the exponent in Eq. (2.22) can decrease to a level that cannot maintain  $\beta \gg 1$ , effectively inhibiting  $Y_\phi$  from further decreasing. Solving  $\beta = 1$  with respect to  $Y_\phi$  and assuming that the variation of  $H$  is small during this rapid process (i.e.,  $H \simeq H_I$ ), we obtain

$$Y_\phi^{(\text{stable})} \simeq \frac{H_I m_\phi^4}{\pi \mu^2 n_{\phi I}} \ln \left( \frac{32\pi H_I m_\phi}{\mu^2} \right), \quad (2.24)$$

which is the stable value of  $Y_\phi$  after rapid depletion. In addition,  $\beta = 1$  can be translated to a critical value of  $\mu$ , denoted by  $\mu_c$ , given by

$$\mu_c^2 = \frac{m_\phi^5}{3\pi M_P^2 H_I} \mathcal{W}_0 \left[ \frac{96\pi^2 M_P^2 H_I^2}{m_\phi^4} \right], \quad (2.25)$$

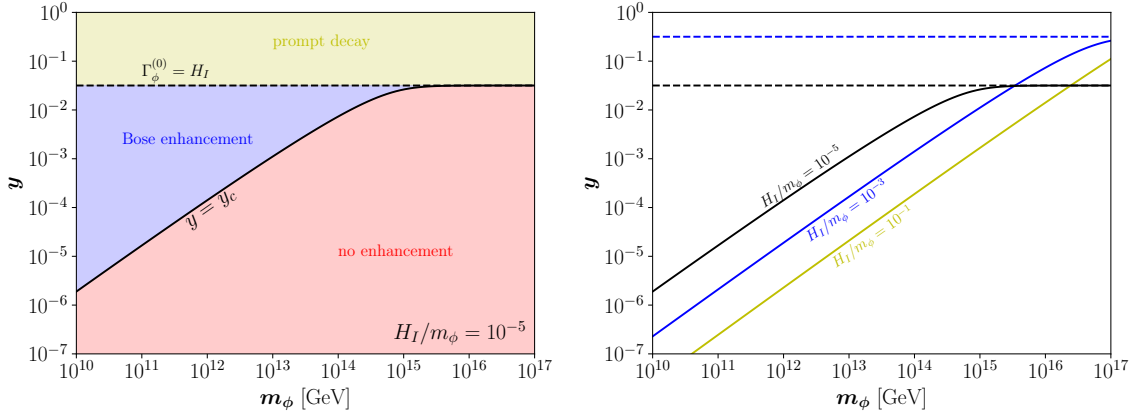


**Figure 3.** Critical value of  $y_c \equiv \mu_c/m_\phi$  (solid lines) and  $\Gamma_\phi^{(0)} = H_I$  (dashed lines), for different values of  $H_I/m_\phi = 10^{-5}$  (black),  $H_I/m_\phi = 10^{-3}$  (blue), or  $H_I/m_\phi = 10^{-1}$  (yellow). For  $y < y_c$  (red area) the inflaton decays without a sizable Bose enhancement, while for  $\Gamma_\phi^{(0)} > H_I$  (yellow area) its decay is prompt even without Bose enhancement. In between, inflatons have a Bose-enhanced decay (blue area).

with  $\mathcal{W}_0$  the principal branch of the Lambert function. For the benchmark values of  $m_\phi$  and  $H_I$  used in Fig. 2, we have  $\mu_c/m_\phi \simeq 2.07 \times 10^{-5}$ , implying that the orange and green lines have  $\mu > \mu_c$ . According to Eq. (2.24), the corresponding values of  $Y_\phi^{(\text{stable})}$  are 0.88 and 0.62, in good agreement with the numerical results in Fig. 2.

In the left panel of Fig. 3, the black solid line shows the critical value of  $y_c \equiv \mu_c/m_\phi$  as a function of the inflaton mass  $m_\phi$ , assuming  $H_I/m_\phi = 10^{-5}$ . Above this line, Bose enhancement leads to exponentially fast decay of the inflaton (cf. the lower panel of Fig. 1), whereas below, the inflaton decays are non-enhanced (cf. the upper panel of Fig. 1). In the small-mass regime, we find  $\mu_c^2 \propto m_\phi^5/(M_P^2 H_I)$ , up to a mild logarithmic correction arising from  $\mathcal{W}_0$  in Eq. (2.25), implying  $y_c \propto m_\phi^{3/2}/(M_P H_I^{1/2})$ . As  $m_\phi$  increases,  $\mathcal{W}_0(96\pi^2 M_P^2 H_I^2/m_\phi^4) \rightarrow 96\pi^2 M_P^2 H_I^2/m_\phi^4$ , and consequently  $\mu_c^2 \rightarrow 32\pi H_I m_\phi$ . As a result,  $y_c \rightarrow (32\pi H_I/m_\phi)^{1/2} = (H_I/\Gamma_\phi^{(0)})^{1/2}$ , as indicated by the horizontal dashed line labeled  $\Gamma_\phi^{(0)} = H_I$ . Above this line, inflaton decay promptly, in a time shorter than a Hubble time, even without Bose enhancement. The right panel of Fig. 3 is similar to the left panel, but overlays the cases  $H_I/m_\phi = 10^{-1}$  and  $H_I/m_\phi = 10^{-3}$ .

In this work, we focus on the scenario with  $\mu > \mu_c$ , i.e., the lower panel of Fig. 1. It is interesting to note that after the Bose-enhanced two-body decay  $\phi \rightarrow \varphi\varphi$  (B2) effectively stops and  $Y_\phi$  reaches  $Y_\phi^{(\text{stable})}$  given by Eq. (2.24), another Bose-enhanced decay process,  $\phi \rightarrow \varphi\varphi h$  with  $h$  the graviton, may take over and further deplete inflatons. This is represented by ‘‘B3: Bose-enhanced 3-body decay’’ in the lower panel of Fig. 1 and will be discussed in detail in the next section.

### 3 Production of gravitational waves

The Bose-enhanced decay of the inflaton not only alters the reheating dynamics, as investigated in the previous section, but also leads to novel GW signatures. In this section, we compute the production of gravitons ( $h$ ) from the following processes<sup>2</sup>

$$\begin{aligned}\varphi\varphi &\rightarrow hh, \\ \phi &\rightarrow \varphi\varphi h, \\ \varphi\phi &\rightarrow \varphi h, \\ \phi\phi &\rightarrow hh,\end{aligned}$$

in which inflatons and reheatons can self-annihilate, coannihilate, or decay. We consider all possible tree-level diagrams with at most four external particles that include at least one graviton. In addition, throughout this section, we assume  $\mu > \mu_c$ .

As preliminary general comments, we note that the first process  $\varphi\varphi \rightarrow hh$  tends to be independent of  $\mu$  as long as  $\mu \gg \mu_c$ . The other three processes depend on the population of the residual particles  $\phi$ , which is roughly proportional to  $\mu^{-2}$ , as suggested by Eq. (2.24). For  $\phi \rightarrow \varphi\varphi h$  and  $\varphi\phi \rightarrow \varphi h$ , although both have  $\varphi$  in the final states, only the former can be Bose enhanced. The latter produces  $\varphi$  with  $p_\varphi$  always above  $m_\phi/2$  while the momentum distribution of the background particles  $\varphi$  peaks at  $p_\varphi \simeq \frac{m_\phi}{2} \frac{a_I}{a}$ .

Since all of these processes are suppressed by the Planck mass scale, they are far from reaching equilibrium. Hence, their impact on the major component of the background (i.e., reheatons) is negligible. However, as we will show later, the residual population of inflatons is further reduced because of its Bose-enhanced three-body decay.

#### 3.1 General formalism

The production of gravitons from the processes mentioned above can be computed by solving the Boltzmann equation (2.11) for the graviton phase-space distribution  $f_h$ . Since  $f_h \ll 1$  is always satisfied in this work, one can safely ignore all terms proportional to  $f_h$  and define the production rate  $\Gamma_h$

$$\Gamma_h(a, p_h) \equiv \lim_{f_h \rightarrow 0} \mathcal{C}[f_h]. \quad (3.1)$$

This allows us to rewrite Eq. (2.11) into the integral form as [25]

$$f_h(a, p_h) = \int_{a_I}^a \frac{da'}{a' H(a')} \Gamma_h \left( a', p_h \frac{a}{a'} \right). \quad (3.2)$$

In the present Universe, the produced gravitons are highly red-shifted, forming a GW background with the following energy density and differential energy density

$$\rho_{\text{GW}} = g_h \int \frac{4\pi \omega^3 d\omega}{(2\pi)^3} f_h(a_0, \omega), \quad (3.3)$$

---

<sup>2</sup>For the Feynman diagrams of these processes and their corresponding amplitudes and production rates, we refer to Ref. [25].

$$\frac{d\rho_{\text{GW}}}{d\omega} = g_h \frac{4\pi \omega^3}{(2\pi)^3} f_h(a_0, \omega), \quad (3.4)$$

where  $\omega$  is the graviton energy,  $g_h = 2$  denotes the two degrees of freedom for massless gravitons, and  $a_0$  is the scale factor at present. It is customary to express the differential energy density in terms of  $\Omega_{\text{GW}}$  which is defined as

$$\Omega_{\text{GW}}(f) \equiv \frac{1}{\rho_c} \frac{d\rho_{\text{GW}}}{d\ln\omega} = 16\pi^2 \frac{f^4}{\rho_c} f_h(a_0, 2\pi f), \quad (3.5)$$

where  $f \equiv \frac{\omega}{2\pi}$  is the GW frequency and  $\rho_c \simeq 1.05 \times 10^{-5} h^2 \text{ GeV/cm}^3$  is the critical energy density at present [35]. At high frequencies, GWs are mainly constrained by the effective number of neutrino species ( $N_{\text{eff}}$ ) from the CMB and BBN observations. The contribution of GWs to  $N_{\text{eff}}$ , denoted by  $\Delta N_{\text{eff}}$ , is proportional to  $\rho_{\text{GW}}$  and is given by

$$\Delta N_{\text{eff}} = \frac{3}{\Omega_\nu} \frac{\rho_{\text{GW}}}{\rho_c}, \quad (3.6)$$

with  $\Omega_\nu \equiv \rho_\nu/\rho_c \simeq 1.7 \times 10^{-5}/h^2$ , where  $\rho_\nu$  is the energy density of the cosmic neutrino background assuming massless neutrinos. Therefore, a bound on  $\Delta N_{\text{eff}}$  can be recast as a bound on  $\Omega_{\text{GW}}$  by [36]

$$\Omega_{\text{GW}} \equiv \frac{\rho_{\text{GW}}}{\rho_c} = \frac{\Omega_\nu}{3} \Delta N_{\text{eff}} \simeq 5.7 \times 10^{-6} h^{-2} \Delta N_{\text{eff}}. \quad (3.7)$$

A subtle issue regarding the consistency between  $\Omega_{\text{GW}} \equiv \rho_{\text{GW}}/\rho_c$  used in Eq. (3.7) and  $\Omega_{\text{GW}}(f) \equiv \frac{1}{\rho_c} \frac{d\rho_{\text{GW}}}{d\ln\omega}$  used in Eq. (3.5) is to be clarified here. The latter is essentially a differential distribution of GW energies with respect to  $\ln\omega$  or  $\ln f$  while the former concerns the total energy density. Strictly speaking, the two  $\Omega_{\text{GW}}$  are different and should be represented by different notation (e.g,  $d\Omega_{\text{GW}}/d\ln f$  versus  $\Omega_{\text{GW}}$ ). However, following the convention in the literature, we use the same notation for both and keep in mind that the two can be distinguished by whether they are  $f$ -dependent. In addition, for a GW spectrum with an  $\mathcal{O}(1)$  span of  $\ln f$ , we roughly have  $\int \Omega_{\text{GW}}(f) d\ln f \sim \mathcal{O}(1) \times \Omega_{\text{GW}}$ , which implies that  $\Omega_{\text{GW}}(f)$  and  $\Omega_{\text{GW}}$  can be interchangeably used up to an  $\mathcal{O}(1)$  factor.

In Fig. 4, we show the sensitivity curves of several proposed GW detectors; these include the Laser Interferometer Space Antenna (LISA) [37], the Einstein Telescope (ET) [38–41], the Cosmic Explorer (CE) [42], the Big Bang Observer (BBO) [43–45], and the ultimate DECIGO (uDECIGO) [46, 47]. We note that the energy stored in the GWs behaves as dark radiation, contributing to the effective number of neutrino species,  $N_{\text{eff}}$ . In order to illustrate these constraints, we include horizontal dashed red lines in Fig. 4. The Planck experiment provides a 95% CL measurement of  $N_{\text{eff}} = 2.99 \pm 0.34$  [48]. Future experiments, such as Simons Observatory (SO) [49, 50], CMB-S4 [51, 52], and CMB-HD [53] are capable of probing  $\Delta N_{\text{eff}}$  above 0.10, 0.06 and 0.028 at  $2\sigma$  C.L., respectively. Some proposed experiments such as COrE [54] and Euclid [55] may reach 0.013 at  $2\sigma$  C.L. In Fig. 4, we selectively plot the limits of some of these experiments. Additionally, we include a limit of  $\Delta N_{\text{eff}} \lesssim 3 \times 10^{-6}$ , reported in Ref. [56], based on a hypothetical cosmic-variance-limited (CVL) CMB polarization experiment.

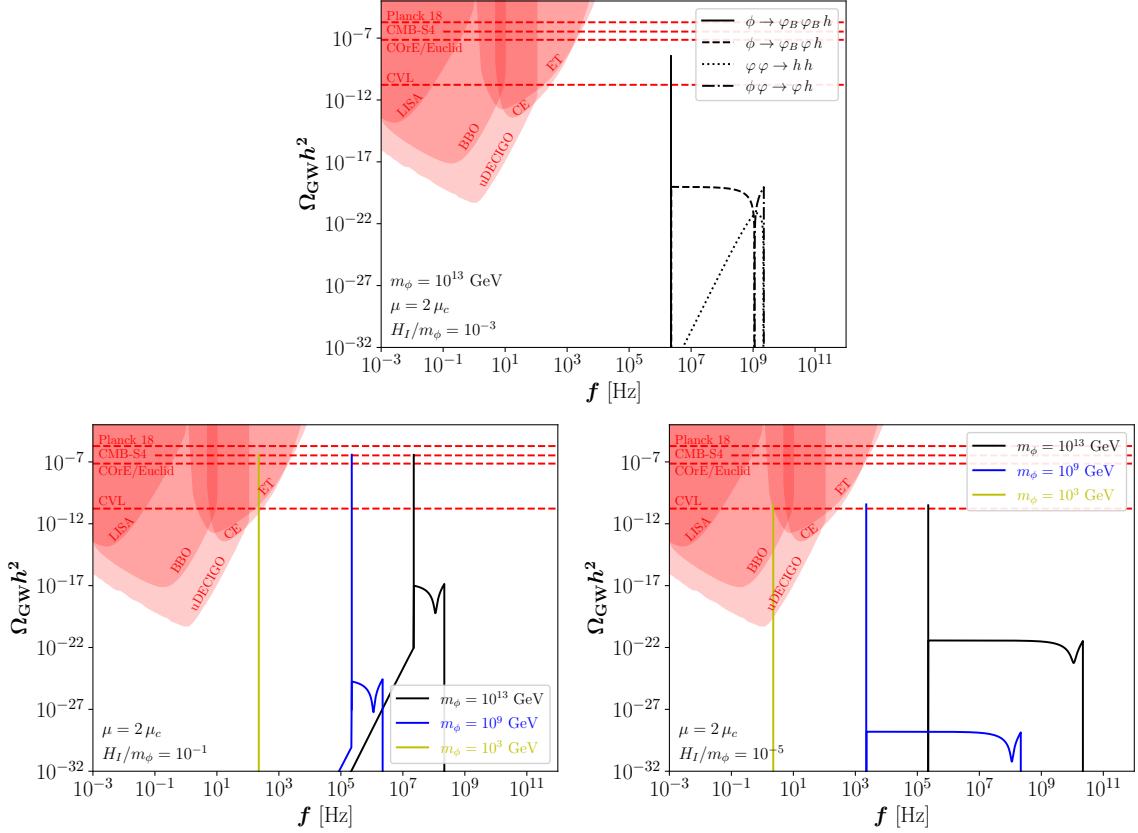


**Figure 4.** Top panel: Individual contributions to the GW spectrum, for  $m_\phi = 10^{13}$  GeV,  $\mu = 2 \mu_c$  and  $H_I/m_\phi = 10^{-3}$ . Here, the subscript  $B$  indicates that it is Bose-enhanced. Lower panels: Total GW spectra for  $H_I/m_\phi = 10^{-1}$  (left) or  $H_I/m_\phi = 10^{-5}$  (right), different inflaton masses, and  $\mu = 2 \mu_c$ . Contributions from  $\phi \rightarrow \varphi \varphi h$  and  $\phi \varphi \rightarrow hh$  are not included due to their weak signal strength—see Eq. (3.35) and Eq. (3.41).

In the top panel of Fig. 4, we also show examples of individual contributions to the GW spectrum for  $m_\phi = 10^{13}$  GeV,  $\mu = 2 \mu_c$  and  $H_I/m_\phi = 10^{-3}$ . Here, the subscript  $B$  indicates that it is Bose-enhanced. In the lower panels, we show the total GW spectra for  $H_I/m_\phi = 10^{-1}$  (left) or  $H_I/m_\phi = 10^{-5}$  (right), different inflaton masses, and  $\mu = 2 \mu_c$ . In the following, we present the calculations and discussion of each specific process.

### 3.2 $\varphi \varphi \rightarrow hh$

For gravitons produced by a pair of massless  $\varphi$  particles, the squared amplitude reads [25, 57]

$$|\mathcal{M}_{\varphi \varphi \rightarrow hh}|^2 = \frac{2 t^2 (s+t)^2}{M_P^4 s^2}, \quad (3.8)$$

where  $s$  and  $t$  are the Mandelstam variables. Plugging the squared amplitude into the corresponding collision term and performing the phase space integration (see Appendix C),

we obtain

$$\Gamma_h^{\varphi\varphi \rightarrow hh} \simeq \frac{\pi n_\varphi^2(a)}{30 M_P^4 p_h x_a} F_1(x_a) \Theta[0 < x_a < 2], \quad (3.9)$$

with  $x_a \equiv (2 p_h / m_\phi) a / a_I$ , and

$$\begin{aligned} F_1(x_a) &\equiv \left( 1 - 5x_a + 10x_a^2 - \frac{15x_a^3}{2} + \frac{15x_a^4}{8} - |1 - x_a|^5 \right) \\ &\simeq \frac{3}{8} (2 - x_a)^3 x_a^3, \end{aligned} \quad (3.10)$$

where the last approximation works within  $\sim 10\%$  precision. The derivation of Eq. (3.9) has used the assumption that the production of  $\varphi$  is instantaneous so that the phase space distribution of  $\varphi$  can be well approximated by the Dirac delta function, i.e.,  $f_\varphi$  is approximately monochromatic. Note that the gravitons produced are not monochromatic, as already indicated by Eq. (3.9).

Substituting Eq. (3.9) into Eq. (3.2), and for a reheaton-dominated scenario

$$H(a) \simeq H_I \left( \frac{a_I}{a} \right)^2, \quad (3.11)$$

we obtain the present value of  $f_h$ :

$$f_h(a_0) \simeq \frac{\pi a_I^2 r_h^3 m_\phi^2}{5 \omega^2} F_1 \left( \frac{2 \omega}{a_I m_\phi} \right), \quad (3.12)$$

where

$$r_h \equiv \frac{H_I}{m_\phi}. \quad (3.13)$$

Here  $a_I$  can be determined by  $\rho_{\text{SM}}(a_\star) a_\star^4 = \rho_I a_I^4$ ,  $\rho_{\text{SM}}(T) = \frac{\pi^2}{30} g_\star(T) T^4$  and  $g_{\star s}(T) T^3 a^3 = g_{\star s}(T_0) T_0^3$  (entropy conservation), where  $\rho_{\text{SM}}$  is the energy density of the SM plasma with temperature  $T$ ,  $a_\star$  denotes the scale factor at the beginning of SM domination, and the subscripts “0” denote present values. From these relations, we obtain

$$a_I \simeq \left( \frac{\pi^2}{30} \right)^{1/4} \frac{g_\star(T_0)^{1/3}}{g_\star^{1/12}} \frac{T_0}{\rho_I^{1/4}} \simeq 2.9 \times 10^{-29} \left( \frac{H_I}{10^{13} \text{ GeV}} \right)^{-\frac{1}{2}}, \quad (3.14)$$

where  $g_\star(T_0) \simeq 3.91$ ,  $T_0 \simeq 2.73$  K, and  $g_{\star s} = g_\star = 106.75$ . It follows that

$$\Omega_{\text{GW}} h^2 \simeq 1.2 \times 10^{-15} \left( \frac{f}{\text{GHz}} \right)^2 \left( \frac{m_\phi}{10^{13} \text{ GeV}} \right) r_h^2 F_1 \left( \frac{2 \omega}{a_I m_\phi} \right), \quad (3.15)$$

where the  $F_1$  part is typically of  $\mathcal{O}(1)$ . The  $\Theta$  function in Eq. (3.9) after cosmological redshift turns into the following interval of  $f$ :

$$0 < f < f_{\text{max}}, \quad (3.16)$$

where

$$f_{\text{max}} \equiv \frac{a_I m_\phi}{2\pi} \simeq 0.071 \text{ GHz} \left( \frac{m_\phi}{10^{13} \text{ GeV}} \frac{1}{r_h} \right)^{\frac{1}{2}}. \quad (3.17)$$

### 3.3 $\phi \rightarrow \varphi \varphi h$

Next, consider the three-body decay  $\phi \rightarrow \varphi \varphi h$ , with the squared amplitude [25]

$$|\mathcal{M}_{\phi \rightarrow \varphi \varphi h}|^2 = \frac{2\mu^2}{M_P^2} \left(1 - \frac{m_\phi}{2\omega}\right)^2. \quad (3.18)$$

From Eq. (3.18), one can compute the corresponding GW production rate  $\Gamma_h$ . Its contribution of the three-body process to the total decay rate of  $\phi$  is determined by

$$\Gamma_\phi^{(3)} = \frac{1}{n_\phi} \int \Gamma_h(\omega) \frac{4\pi\omega^2}{(2\pi)^3} d\omega. \quad (3.19)$$

It is important to note that the integral in Eq. (3.19) is IR divergent. This feature is very common in particle physics processes containing bremsstrahlung of soft massless bosons (e.g.  $Z \rightarrow e^+e^-\gamma$ ,  $e^- + N \rightarrow e^- + N + \gamma$ ). In Minkowski spacetime with zero temperature, such IR divergences are regulated by cancelation with associated loop processes—see, e.g., Ref. [58]. For gravitons, a similar cancelation has also been studied [59]. In a finite-density environment, cancelation between emission and absorption processes can occur [60, 61], if the mean free path of gravitons, which decreases with decreasing frequency in the IR limit, is sufficiently short to render the environment opaque to very soft gravitons. In the early Universe with a rapid expansion rate, QFT calculations based on Minkowski spacetime are valid only when the relevant length scale is shorter than the horizon radius  $\sim 1/H$ . Therefore, the horizon itself provides an IR cutoff [11]:

$$\omega > H. \quad (3.20)$$

The physical interpretation of this cutoff is clear: no waves with wavelengths longer than the size of a causally connected part of the Universe can be generated. We have checked that in our work the cutoff in Eq. (3.20) is well above the scale relevant to the cancelation discussed in Refs. [60, 61]. Hence, Eq. (3.20) will be used as the cutoff in the following calculation.

When computing the collision term of  $\phi \rightarrow \varphi \varphi h$ , three contributions are encountered, from double Bose-enhanced decay ( $\phi \rightarrow \varphi_B \varphi_B h$ , with the subscript “ $B$ ” indicating that it is Bose-enhanced), single Bose-enhanced decay ( $\phi \rightarrow \varphi_B \varphi h$ ), and decay without any enhancement. The detailed calculations of these contributions are presented in the Appendix C. It turns out that  $\phi \rightarrow \varphi_B \varphi_B h$  leads to the highest yield of gravitons produced in this work and has the strongest impact on the background among the three decay processes, as will be described in the following.

#### 3.3.1 $\phi \rightarrow \varphi_B \varphi_B h$

Let us start with the double Bose-enhanced contribution  $\phi \rightarrow \varphi_B \varphi_B h$ . Assuming that the background  $\varphi$  particles is monochromatic, it is straightforward to perform the phase space integration of the collision term (see Appendix C for details) and obtain

$$\Gamma_h^{\phi \rightarrow \varphi_B \varphi_B h} \simeq \frac{4\pi^3 \mu^2 n_\varphi^2 n_\phi}{m_\phi^5 M_P^2 \omega^2} \left(1 - \frac{m_\phi}{2\omega}\right)^2 \left(\frac{a}{a_I}\right)^4 \delta(\omega_B - \omega) \Theta[\omega_B > H], \quad (3.21)$$

where  $\omega_B \equiv m_\phi (1 - a_I/a)$ . As indicated in Eq. (3.21), this process produces a monochromatic graviton because the energies of  $\phi$  and two  $\varphi_B$  are fixed.

Substituting Eq. (3.21) into Eq. (3.19), we obtain

$$\Gamma_\phi^{(3)} \simeq \frac{2\pi \mu^2 n_\varphi^2}{m_\phi^5 M_P^2} \left( \frac{a}{a_I} \right)^4 \left( 1 - \frac{m_\phi}{2\omega_B} \right)^2 \Theta [\omega_B > H]. \quad (3.22)$$

Note that if  $a = a_I$ ,  $\omega_B = 0$  is below  $H$ , leading to a vanishing result. The function  $\Theta$  becomes nonzero when  $a$  exceeds a certain threshold, indicated by  $a_3$  and shown diagrammatically in Fig. 1. By solving  $\omega_B = H$  with  $H = H_I(a_I/a_3)^2$  and  $\omega_B = m_\phi(1 - a_I/a_3)$ , we get

$$a_3 = a_I \frac{1 + \sqrt{1 + 4r_h}}{2}. \quad (3.23)$$

When  $\omega_B > H$  (i.e.  $a > a_3$ ), one can compare  $\Gamma_\phi^{(3)}$  to  $H$ . Assuming  $r_h \ll 1$ , the ratio of  $\Gamma_\phi^{(3)}$  to  $H$  reads

$$\frac{\Gamma_\phi^{(3)}}{H} \simeq 1.3 \times 10^2 \left( \frac{y}{y_c} \right)^2 \gg 1, \quad (3.24)$$

where we have approximated  $n_\varphi \simeq 2n_{\phi I}(a_I/a)^3$ . Equation (3.24) implies that once  $a > a_3$  is satisfied, the remaining  $\phi$  particles would decay rapidly via  $\phi \rightarrow \varphi_B \varphi_B h$  (corresponding to the “B3” turning point in Fig. 1). Since  $\Gamma_\phi^{(3)}$  is at least two orders of magnitude above  $H_I$ , it is a good approximation to assume that this decay is instantaneous. Under this assumption, the total energy of gravitons produced after the instantaneous decay is given by

$$\rho_h^{\phi \rightarrow \varphi_B \varphi_B h} \simeq n_{\phi I} Y_\phi^{(\text{stable})} \omega_B \left( \frac{a_I}{a} \right)^4, \quad (3.25)$$

where  $\omega_B \simeq H_I(1 - 2r_h)$ . Using Eqs. (2.24), (3.7) and (3.14), we can rewrite Eq. (3.25) as

$$\Omega_{\text{GW}} h^2 \simeq 1.8 \times 10^{-8} \left( \frac{m_\phi}{10^{13} \text{ GeV}} \frac{4 \times 10^{-5}}{y} \right)^2 \ln \left( \frac{32\pi r_h}{y^2} \right). \quad (3.26)$$

This is a monochromatic spectrum (the solid vertical lines shown in Fig. 4), with frequency  $f = r_h f_{\text{max}}$  where  $f_{\text{max}}$  is defined in Eq. (3.17).

Equation (3.25) can be reinterpreted in terms of  $\Delta N_{\text{eff}}$  as

$$\Delta N_{\text{eff}} \simeq 0.13 \left( \frac{y_c}{y} \right)^2 r_h \ln \left( \frac{32\pi r_h}{y^2} \right). \quad (3.27)$$

It is interesting to note that the resulting  $\Delta N_{\text{eff}}$  is close to the current bound set by the Planck experiment and can be probed by future experiments. For example, if we take  $m_\phi = 10^{13}$  GeV,  $r_h = 0.1$ , and  $y = 1.7 y_c$ , we obtain  $\Delta N_{\text{eff}} \simeq 0.1$ , which could be reached by next-generation observatories such as CMB-S4.

### 3.3.2 $\phi \rightarrow \varphi_B \varphi h$

The single Bose-enhanced decay has a lower graviton yield compared with the double Bose-enhanced decay, but it produces a continuous GW spectrum, as opposed to the monochromatic spectrum discussed above. Performing the phase space integration (see Appendix C for details), we obtain the corresponding collision term

$$\Gamma_h^{\phi \rightarrow \varphi_B \varphi h} \simeq \frac{\pi \mu^2 n_\varphi n_\phi}{2 m_\phi^3 M_P^2 \omega^2} \left(1 - \frac{m_\phi}{2\omega}\right)^2 \left(\frac{a}{a_I}\right)^2. \quad (3.28)$$

Substituting Eq. (3.28) into Eq. (3.2), we obtain

$$f_h \simeq \frac{3\pi \mu^2 H_I n_{\phi I} Y_\phi^{(\text{stable})}}{8 m_\phi^2 \omega^4 r_a^4} [(r_a - 1)(1 + r_a - 4x_a) + 2x_a^2 \ln r_a], \quad (3.29)$$

where  $r_a \equiv a/a_I$ . Note that Eq. (3.29) is valid only when the comoving number density of  $\phi$  is constant. When  $a \simeq a_3$ , the remaining inflatons are rapidly depleted via  $\phi \rightarrow \varphi_B \varphi h$ . Therefore, to compute the GW spectrum today from  $\phi \rightarrow \varphi_B \varphi h$ , we should cut the production at  $a = a_3$  and then redshift  $f_h(a = a_3)$  to the present ( $a = a_0$ ). Using Eq. (3.23) with the approximation  $r_h \ll 1$ , we get

$$f_h(a_0, \omega) \simeq \frac{3 a_I^2 m_\phi^2 r_h^3}{\omega^2} \left(1 - \frac{a_I m_\phi}{2\omega}\right)^2 \ln\left(\frac{32\pi r_h}{y^2}\right) \Theta\left(r_h < \frac{\omega}{a_I m_\phi} < \frac{1}{2}\right). \quad (3.30)$$

The corresponding GW spectrum is

$$\Omega_{\text{GW}} h^2 \simeq 5.5 \times 10^{-15} \left(\frac{f}{\text{GHz}}\right)^2 \left(\frac{m_\phi}{10^{13} \text{ GeV}}\right) r_h^2 \left(\frac{f_{\text{max}}}{2f} - 1\right)^2 \ln\left(\frac{32\pi r_h}{y^2}\right), \quad (3.31)$$

and spans over the following frequency band

$$r_h f_{\text{max}} < f < \frac{1}{2} f_{\text{max}}. \quad (3.32)$$

### 3.3.3 $\phi \rightarrow \varphi \varphi h$

It is also possible to produce gravitons through a three-body process without any Bose enhancement. The contribution to the GW spectra is expected to be subdominant compared to the previous two cases with Bose enhancement. Indeed, the collision term for the process  $\phi \rightarrow \varphi \varphi h$  is given by [25]

$$\Gamma_h^{\phi \rightarrow \varphi \varphi h} = \frac{\mu^2 n_\phi}{32\pi M_P^2 m_\phi \omega} \left(1 - \frac{m_\phi}{2\omega}\right)^2, \quad (3.33)$$

which is suppressed by a factor of  $\frac{\omega m_\phi^2}{n_\varphi}$  compared to Eq. (3.28) for  $\phi \rightarrow \varphi_B \varphi h$ . This factor is suppressed by the smallness of  $\mu$ , as can be seen in  $\frac{\omega m_\phi^2}{n_\varphi} < \frac{m_\phi^3}{n_\varphi} < \frac{m_\phi^3}{n_{\phi I} Y_\phi^{(\text{stable})}} \sim \frac{\mu^2}{H_I m_\phi} \ll 1$ . Such suppression is also reflected in the corresponding GW spectrum. Substituting Eq. (3.33) into Eq. (3.2), we find

$$f_h \simeq \frac{\mu^2 m_\phi n_{\phi I} Y_\phi^{(\text{stable})}}{256\pi H_I M_P^2 \omega^3 r_a^3} [(r_a - 1)(1 + r_a - 4x_a) + 2x_a^2 \ln r_a], \quad (3.34)$$

and the GW amplitude at present is given by

$$\Omega_{\text{GW}} h^2 \simeq 1.4 \times 10^{-27} \left( \frac{f}{\text{GHz}} \right)^3 \left( 1 - \frac{f_{\text{max}}}{2f} \right)^2 r_h^{1/2} \left( \frac{m_\phi}{10^{13} \text{ GeV}} \right)^{5/2} \ln \left( \frac{32\pi r_h}{y^2} \right). \quad (3.35)$$

The frequency band is the same as in Eq. (3.32). It is evident that Eq. (3.35) is significantly smaller than Eq. (3.31) for the same model parameters. We also note that, for  $f \ll f_{\text{max}}$ , the spectrum scales as  $\Omega_{\text{GW}} \propto f$ , which is a characteristic feature of bremsstrahlung graviton production.

### 3.4 $\varphi\phi \rightarrow \varphi h$

The scattering process  $\varphi\phi \rightarrow \varphi h$  is expected to have a graviton yield comparable to that of the single Bose-enhanced decay  $\phi \rightarrow \varphi_B \varphi h$ . The Bose enhancement in the latter plays a role equivalent to the presence of an initial-state  $\varphi$  with large  $f_\varphi$  in the former. Moreover, they share the same squared matrix element, which follows from crossing symmetry—see Ref. [26] for more detailed discussions. Nevertheless, a difference in the symmetry factor should be taken into account—see Tab. 1 of Ref. [25]. The resulting collision term is

$$\Gamma_h^{\varphi\phi \rightarrow \varphi h} \simeq \frac{\pi \mu^2 n_\varphi n_\phi}{2 m_\phi^3 M_P^2 \omega^2} \left( 1 - \frac{m_\phi}{2\omega} \right)^2 \left( \frac{a}{a_I} \right)^2 \Theta \left[ \frac{1}{2} < \frac{\omega}{m_\phi} < 1 \right]. \quad (3.36)$$

The corresponding  $f_h$  is very similar to Eq. (3.30), except for a different  $\Theta$  function:

$$f_h(a=1) \simeq \frac{3 a_I^2 m_\phi^2 r_h^3}{\omega^2} \left( 1 - \frac{a_I m_\phi}{2\omega} \right)^2 \ln \left( \frac{32\pi r_h}{y^2} \right) \Theta \left( \frac{1}{2} < \frac{\omega}{a_I m_\phi} < 1 \right). \quad (3.37)$$

Consequently, the expression for  $\Omega_{\text{GW}} h^2$  in Eq. (3.31) can be used with the following frequency band

$$\frac{1}{2} f_{\text{max}} < f < f_{\text{max}}. \quad (3.38)$$

### 3.5 $\phi\phi \rightarrow hh$

Finally, gravitons can also be produced from inflaton pair annihilation [21, 22]. The corresponding collision term is given by [25]

$$\Gamma_h^{\phi\phi \rightarrow hh} = \frac{\pi}{16} \frac{n_\phi^2}{M_P^4} \delta(\omega - m_\phi). \quad (3.39)$$

This channel also produces gravitons monochromatically; however, the resulting GW amplitude is typically small due to the additional Planck-scale suppression and low inflaton density drained by the Bose enhanced two-body decay. Plugging Eq. (3.39) into Eq. (3.2), we find

$$f_h \simeq \frac{H_I m_\phi^{11}}{16 \pi M_P^4 \mu^4 r_a^4 \omega^4} \ln \left( \frac{32\pi r_h}{y^2} \right), \quad (3.40)$$

for  $a \lesssim a_3$ . The GW amplitude at present is given by

$$\Omega_{\text{GW}} h^2 \simeq 2.0 \times 10^{-23} \left( \frac{m_\phi}{10^{13} \text{ GeV}} \right)^6 r_h^{-1} \left( \frac{4 \times 10^{-5}}{y} \right)^4 \ln \left( \frac{32\pi r_h}{y^2} \right), \quad (3.41)$$

which corresponds to a very narrow spectrum with  $f \simeq f_{\max}$  since the inflaton energy would be almost completely drained by the Bose enhanced three-body process at  $a \simeq a_3$ . We remind the reader that in scenarios where graviton pair production from inflaton annihilation occurs during a matter-dominated phase, with  $H \propto a^{-3/2}$ , the resulting GW spectrum typically exhibits the scaling  $\Omega_{\text{GW}} h^2 \propto f^{-1/2}$ , see, e.g., Refs. [21, 22, 24–26]. In contrast, the production considered here takes place during a radiation-dominated era driven by massless  $\varphi$  particles. This difference in the background expansion history explains the distinct frequency scaling of the GW spectrum compared to the results in the literature.

## 4 Conclusions

In this work, we propose a novel reheating scenario in which the bosonic decay products of the inflaton—dubbed the reheaton—form a transient condensate with a large occupation number. Due to Bose enhancement effects, two-body inflaton decays can proceed much more efficiently than in conventional perturbative reheating scenarios, leading to a rapid transfer of energy from inflatons to radiation (reheatons), as illustrated schematically in Fig. 1. This enhancement accelerates the overall reheating process and modifies the inflaton decay dynamics in a way that is not captured by standard treatments. We show that once the inflaton-reheaton coupling exceeds a critical value given by Eq. (2.25), the inflaton almost immediately transfers a significant fraction of its energy to the reheaton at the beginning of reheating, as quantitatively demonstrated in Fig. 2.

In addition to altering the standard two-body decay channels of the inflaton, we have shown that the formation of a reheaton condensate can dramatically enhance graviton production during reheating. In particular, inflaton three-body decays with a graviton in the final state are strongly amplified by Bose enhancement, owing to the large occupation number of the condensate. While such processes are ordinarily suppressed by powers of the Planck scale, we find that Bose enhancement can compensate for this suppression, rendering the corresponding decay rate comparable to—or even exceeding—the Hubble expansion rate. As a result, these three-body channels can also play a significant role in further depleting the inflaton energy density during reheating. At the same time, the enhanced graviton emission associated with these processes leads to a substantial amplification of the resulting stochastic gravitational-wave (GW) background compared to scenarios without Bose enhancement. Moreover, the resulting GW spectra exhibit characteristic features associated with the reheating dynamics and the presence of the condensate. The corresponding stochastic GW signal can reach levels potentially accessible to future experiments, as illustrated in Fig. 4.

In summary, we have proposed a novel perturbative reheating scenario in which quantum-statistical effects play an important role in energy transfer and graviton production. Our analysis shows that transient reheaton condensation can enhance inflaton decay rates and amplify GW emission, thereby providing an alternative mechanism that may lead to observable consequences.

## Acknowledgments

We thank Wen-Yuan Ai, Anna Tokareva, and Jing-Zhi Zhou for very useful discussions on the IR divergence and the horizon cutoff. NB thanks the Laboratoire d'Annecy-le-Vieux de Physique Théorique (LAPTh) for its hospitality and CNRS-INP for partial support. XJX thanks the high energy physics group at New York University Abu Dhabi for their hospitality—and for the opportunity to ride a camel—during a short-term visit, where part of this project was carried out. NB received funding from the grants PID2023-151418NB-I00 funded by MCIU/AEI/10.13039 /501100011033/ FEDER and PID2022-139841NB-I00 of MCIU/AEI/10.13039/501100011033 and FEDER, UE. XJX is supported in part by the National Natural Science Foundation of China under grant No. 12141501 and also by the CAS Project for Young Scientists in Basic Research (YSBR-099). YX has received support from the Natural Sciences and Engineering Research Council (NSERC) of Canada.

## A Phase space integrals for the 1-to-2 process

For  $\phi \rightarrow \varphi\varphi$ , which has a constant squared matrix element  $|\mathcal{M}|^2 = \mu^2$ , the full expressions of the collision terms  $\mathcal{C}[f_\phi]$  and  $\mathcal{C}[f_\varphi]$  are

$$\mathcal{C}[f_\phi] \equiv \frac{1}{2E_\phi} \frac{\mu^2}{2} \int d\Pi_2 d\Pi_3 (2\pi\delta)^4 [-f_\phi (1+f_2)(1+f_3) + f_2 f_3 (1+f_\phi)], \quad (\text{A.1})$$

$$\mathcal{C}[f_\varphi] \equiv \frac{1}{2E_\varphi} \mu^2 \int d\Pi_1 d\Pi_3 (2\pi\delta)^4 [-f_\varphi f_3 (1+f_1) + f_1 (1+f_\varphi)(1+f_3)], \quad (\text{A.2})$$

where the subscripts 1, 2, and 3 denote quantities for the 1<sup>st</sup>, 2<sup>nd</sup>, and 3<sup>rd</sup> particles in  $\phi \rightarrow \varphi\varphi$ , respectively. In the expression of  $\mathcal{C}[f_\varphi]$ , we assign the 2<sup>nd</sup> particle to the one considered on the left-hand side of the Boltzmann equation. The notation  $(2\pi\delta)^4$  represents the common four-dimensional delta function responsible for momentum conservation.

In Eq. (A.1), after expanding the products of those  $f$ 's and applying the symmetry of  $2 \leftrightarrow 3$ , one finds that the part in the square brackets can be replaced by  $-f_\phi - 2f_\phi f_2 + f_2 f_3$ . In Eq. (A.2), after a similar expansion, we obtain  $f_1 + f_1 f_\varphi + f_1 f_3 - f_\varphi f_3$ . Therefore, we encounter the following phase space integrals:

$$I_A = \frac{1}{2E_\phi} \frac{\mu^2}{2} \int d\Pi_2 d\Pi_3 (2\pi)^4 \delta^{(4)}(p_\phi - p_2 - p_3) f_\phi, \quad (\text{A.3})$$

$$I_B = 2 \times \frac{1}{2E_\phi} \frac{\mu^2}{2} \int d\Pi_2 d\Pi_3 (2\pi)^4 \delta^{(4)}(p_\phi - p_2 - p_3) f_\phi f_2, \quad (\text{A.4})$$

$$I_C = \frac{1}{2E_\phi} \frac{\mu^2}{2} \int d\Pi_2 d\Pi_3 (2\pi)^4 \delta^{(4)}(p_\phi - p_2 - p_3) f_2 f_3, \quad (\text{A.5})$$

$$I_D = \frac{1}{2E_\varphi} \mu^2 \int d\Pi_1 d\Pi_3 (2\pi)^4 \delta^{(4)}(p_1 - p_\varphi - p_3) f_1, \quad (\text{A.6})$$

$$I_{E1} = \frac{1}{2E_\varphi} \mu^2 \int d\Pi_1 d\Pi_3 (2\pi)^4 \delta^{(4)}(p_1 - p_\varphi - p_3) f_1 f_\varphi, \quad (\text{A.7})$$

$$I_{E2} = \frac{1}{2E_\varphi} \mu^2 \int d\Pi_1 d\Pi_3 (2\pi)^4 \delta^{(4)}(p_1 - p_\varphi - p_3) f_1 f_3, \quad (\text{A.8})$$

$$I_F = \frac{1}{2E_\varphi} \mu^2 \int d\Pi_1 d\Pi_3 (2\pi)^4 \delta^{(4)}(p_1 - p_\varphi - p_3) f_\varphi f_3. \quad (\text{A.9})$$

Assuming that  $f_\phi$  is a highly nonrelativistic distribution ( $p_\phi \approx 0$ ) and  $\varphi$  always has its momentum  $p_\varphi \leq m_\phi/2$ , the results of these integrals are

$$I_A = \frac{\mu^2}{32\pi E_\phi} f_\phi(p_\phi), \quad (\text{A.10})$$

$$I_B = I_A f_\varphi \left( \frac{m_\phi}{2} \right), \quad (\text{A.11})$$

$$I_C = 0, \quad (\text{A.12})$$

$$I_D = \frac{\pi \mu^2 n_\phi}{2 m_\phi^3} \delta \left( p_\varphi - \frac{m_\phi}{2} \right), \quad (\text{A.13})$$

$$I_{E1} = I_{E2} = \frac{\pi \mu^2 n_\phi}{4 m_\phi^3} \delta \left( p_\varphi - \frac{m_\phi}{2} \right) f_\varphi \left( \frac{m_\phi}{2} \right), \quad (\text{A.14})$$

$$I_F = 0. \quad (\text{A.15})$$

In the following, we present the calculations in detail. Although the specific form of  $f_\phi$  is irrelevant to the final results as long as it is nonrelativistic, it is helpful to assume a simple analytical form of  $f_\phi$ :

$$f_\phi = \lim_{\varepsilon \rightarrow 0^+} 2\pi^2 \frac{n_\phi}{\varepsilon^2} \delta(p_\phi - \varepsilon). \quad (\text{A.16})$$

Equation (A.16) has been properly normalized such that

$$\int f_\phi(p_\phi) \frac{d^3 p_\phi}{(2\pi)^3} = \int \frac{n_\phi}{\varepsilon^2} \delta(p_\phi - \varepsilon) p_\phi^2 dp_\phi = n_\phi. \quad (\text{A.17})$$

First, we compute  $I_A$ :

$$\begin{aligned} I_A &= \frac{\mu^2}{4E_\phi} \int d\Pi_2 d\Pi_3 (2\pi)^4 \delta^{(4)}(p_\phi - p_2 - p_3) f_\phi \\ &= \frac{\mu^2}{64\pi^2 E_\phi} f_\phi \int \frac{d^3 \mathbf{p}_2}{E_2} \frac{1}{E_3} \delta(E_\phi - E_2 - E_3) \bigg|_{E_3 = \sqrt{p_\phi^2 + p_2^2 - 2p_\phi p_2 c_\theta}} \\ &= \frac{\mu^2}{64\pi^2 E_\phi} f_\phi \int \frac{2\pi p_2^2 dp_2 dc_\theta}{p_2} \frac{\delta(E_\phi - E_2 - \sqrt{p_\phi^2 + p_2^2 - 2p_\phi p_2 c_\theta})}{\sqrt{p_\phi^2 + p_2^2 - 2p_\phi p_2 c_\theta}} \\ &= \frac{\mu^2}{32\pi E_\phi} f_\phi \int \frac{p_2^2 dp_2}{p_2} \frac{1}{p_\phi p_2} \Theta \left[ \frac{E_\phi - p_\phi}{2} \leq p_2 \leq \frac{E_\phi + p_\phi}{2} \right] = \frac{\mu^2}{32\pi E_\phi} f_\phi, \end{aligned} \quad (\text{A.18})$$

where  $c_\theta$  is the cosine of the angle between the two  $\varphi$  particles.

Next, we compute  $I_B$ , which is similar to  $I_A$ , except for an additional factor of  $f_\varphi(p_2)$ :

$$I_B = 2 \times \frac{1}{2E_\phi} \frac{\mu^2}{2} f_\phi \int d\Pi_2 d\Pi_3 (2\pi)^4 \delta^{(4)}(p_\phi - p_2 - p_3) f_\varphi(p_2)$$

$$\begin{aligned}
&= 2 \frac{\mu^2}{32\pi E_\phi} f_\phi \int \frac{p_2^2 dp_2}{p_2} \frac{f_\varphi(p_2)}{p_\phi p_2} \Theta \left[ \frac{E_\phi - p_\phi}{2} \leq p_2 \leq \frac{E_\phi + p_\phi}{2} \right] \\
&= 2 I_A \frac{1}{p_\phi} \int_{\frac{E_\phi - p_\phi}{2}}^{\frac{E_\phi + p_\phi}{2}} dp_2 f_\varphi(p_2). \tag{A.19}
\end{aligned}$$

Here, the integral after  $I_A$  can be viewed as the average value of  $f_\varphi$  around  $E_\phi/2$  within a small interval (the width is  $p_\phi$ ). This average value approaches  $f_\varphi(\frac{m_\phi}{2})/2$  if one takes the nonrelativistic approximation in Eq. (A.16) and assumes that  $f_\varphi$  vanishes at  $p_\varphi > m_\phi/2$ . Then the result  $I_B$  is given by Eq. (A.11).

Under the same assumption, the calculation of  $I_C$  leads to a vanishing result:

$$\begin{aligned}
I_C &= \frac{1}{2E_\phi} \frac{\mu^2}{2} \int d\Pi_2 d\Pi_3 (2\pi)^4 \delta^{(4)}(p_\phi - p_2 - p_3) f_2 f_3, \\
&= \frac{\mu^2}{64\pi^2 E_\phi} \int \frac{d^3 \mathbf{p}_2}{E_2} \frac{d^3 \mathbf{p}_3}{E_3} f_\varphi(p_2) f_\varphi(p_3) \delta(E_\phi - E_2 - E_3) \delta^{(3)}(\mathbf{p}_\phi - \mathbf{p}_2 - \mathbf{p}_3) \\
&= \frac{\mu^2}{64\pi^2 E_\phi} \int \frac{d^3 \mathbf{p}_2}{E_2} \frac{f_\varphi(p_2) f_\varphi(p_3)}{E_3} \delta(E_\phi - E_2 - E_3) \Big|_{\mathbf{p}_3 = \mathbf{p}_\phi - \mathbf{p}_2} \\
&= \frac{\mu^2}{64\pi^2 E_\phi} \int \frac{2\pi p_2^2 dp_2 dc_\theta}{p_2} \frac{f_\varphi(p_2) f_\varphi(E_\phi - p_2)}{p_2 p_\phi} \delta \left( c_\theta - \frac{p_\phi^2 - E_\phi^2 + 2E_\phi p_2}{2 p_\phi p_2} \right) = 0. \tag{A.20}
\end{aligned}$$

The vanishing result can be physically understood from the fact that the production of  $\phi$  from two  $\varphi$ 's requires not only  $p_\varphi \geq m_\phi/2$  but also  $c_\theta \rightarrow -1$ . It can also be rigorously proved using Eq. (A.16) with  $\varepsilon \rightarrow 0^+$ .

The calculation of  $I_D$  is given as follows:

$$\begin{aligned}
I_D &= \frac{1}{2E_\varphi} \mu^2 \int d\Pi_1 d\Pi_3 (2\pi)^4 \delta^{(4)}(p_1 - p_\varphi - p_3) f_1 \\
&= \frac{\mu^2}{32\pi^2 E_\varphi} \int \frac{d^3 \mathbf{p}_1}{E_1} \frac{1}{p_3} \delta(E_1 - p_\varphi - p_3) f_\phi(p_1) \Big|_{\mathbf{p}_3 = \mathbf{p}_1 - \mathbf{p}_\varphi} \\
&= \frac{\mu^2}{32\pi^2 E_\varphi} \int \frac{2\pi p_1^2 dp_1 dc_\theta}{E_1} \frac{\delta(E_1 - p_\varphi - \sqrt{p_1^2 + p_\varphi^2 - 2p_1 p_\varphi c_\theta})}{\sqrt{p_1^2 + p_\varphi^2 - 2p_1 p_\varphi c_\theta}} f_\phi(p_1) \\
&= \frac{\mu^2}{16\pi E_\varphi} \int \frac{p_1^2 dp_1}{E_1} \frac{1}{p_1 p_\varphi} f_\phi(p_1) \Theta \left[ \frac{m_\phi^2 - 4p_\varphi^2}{4p_\varphi} \leq p_1 \right] \\
&= \frac{\mu^2}{16\pi E_\varphi^2} \int_0^\infty \frac{p_1 dp_1}{E_1} \frac{2\pi^2 n_\phi}{\varepsilon^2} \delta(p_1 - \varepsilon) \Theta \left[ \frac{m_\phi^2 - 4p_\varphi^2}{4p_\varphi} \leq p_1 \right] \\
&= \frac{\mu^2}{16\pi E_\varphi^2} \frac{2\pi^2 n_\phi}{\sqrt{m_\phi^2 + \varepsilon^2}} \frac{1}{\varepsilon} \Theta \left[ \left| p_\varphi - \frac{1}{2} \sqrt{m_\phi^2 + \varepsilon^2} \right| \leq \frac{\varepsilon}{2} \right] \\
&= \frac{\pi \mu^2 n_\phi}{2 m_\phi^3} \delta \left( p_\varphi - \frac{m_\phi}{2} \right), \tag{A.21}
\end{aligned}$$

where  $c_\theta$  is the cosine of the angle between  $\vec{p}_1$  and  $\vec{p}_\varphi$ .

The calculation of  $I_{E1}$  is simple since  $f_\varphi$  can be factored out of the integral. So, the result is expected to be similar to Eq. (A.21). However, one needs to be careful about a factor of  $1/2$  arising from that the delta function in Eq. (A.21) is symmetric with respect to  $p_\varphi = m_\phi/2$ , while  $f_\varphi$  vanishes if  $p_\varphi > m_\phi/2$ .

If  $f_\varphi$  is replaced by  $f_3 = f_\varphi(p_3)$ ,  $I_{E1}$  changes to  $I_{E2}$ . The calculation is different, but it leads to the same result:

$$\begin{aligned}
I_{E2} &= \frac{\mu^2}{2E_\varphi} \int d\Pi_1 d\Pi_3 (2\pi)^4 \delta^{(4)}(p_1 - p_\varphi - p_3) f_1 f_3 \\
&= \frac{\mu^2}{32\pi^2 E_\varphi} \int \frac{d^3 \mathbf{p}_1}{E_1} \frac{1}{p_3} \delta(E_1 - p_\varphi - p_3) f_\phi(p_1) f_\varphi(p_3) \Big|_{\mathbf{p}_3 = \mathbf{p}_1 - \mathbf{p}_\varphi} \\
&= \frac{\mu^2}{16\pi E_\varphi} \int \frac{p_1^2 dp_1}{E_1} \frac{1}{p_1 p_\varphi} f_\phi(p_1) f_\varphi(E_1 - p_\varphi) \Theta \left[ \frac{m_\phi^2 - 4p_\varphi^2}{4p_\varphi} \leq p_1 \right] \\
&= \frac{\mu^2}{16\pi E_\varphi^2} \int_0^\infty \frac{p_1 dp_1}{E_1} f_\phi(p_1) f_\varphi(E_1 - p_\varphi) \Theta \left[ \frac{m_\phi^2 - 4p_\varphi^2}{4p_\varphi} \leq p_1 \right] \\
&= \frac{\mu^2}{16\pi E_\varphi^2} \int_0^\infty \frac{p_1 dp_1}{E_1} \frac{2\pi^2 n_\phi}{\varepsilon^2} \delta(p_1 - \varepsilon) f_\varphi(E_1 - p_\varphi) \Theta \left[ \frac{m_\phi^2 - 4p_\varphi^2}{4p_\varphi} \leq p_1 \right] \\
&= \frac{\mu^2}{16\pi E_\varphi^2} \frac{2\pi^2 n_\phi}{\sqrt{m_\phi^2 + \varepsilon^2}} f_\varphi \left( \sqrt{m_\phi^2 + \varepsilon^2} - p_\varphi \right) \frac{1}{\varepsilon} \Theta \left[ \left| p_\varphi - \frac{1}{2} \sqrt{m_\phi^2 + \varepsilon^2} \right| \leq \frac{\varepsilon}{2} \right] \\
&= \frac{\pi \mu^2 n_\phi}{4 m_\phi^3} \delta \left( p_\varphi - \frac{m_\phi}{2} \right) f_\varphi \left( \frac{m_\phi}{2} \right), \tag{A.22}
\end{aligned}$$

where we need to take into account a similar factor of  $1/2$  as before.

The calculation of  $I_F$  is similar to that of  $I_C$ , which leads to a vanishing result.

## B Solving the Boltzmann equation of $f_\varphi$

The unintegrated Boltzmann equation of  $f_\varphi$  reads

$$\left( \frac{\partial}{\partial t} - H p_\varphi \frac{\partial}{\partial p_\varphi} \right) f_\varphi(t, p_\varphi) = \frac{16\pi^2 \Gamma_\phi^{(0)} n_\phi}{m_\phi^2} \delta \left( p_\varphi - \frac{m_\phi}{2} \right) \mathcal{B}_e. \tag{B.1}$$

Since  $\mathcal{B}_e$  is multiplied by the  $\delta$  function, one can replace  $\mathcal{B}_e = 1 + f_\varphi \left( t, \frac{m_\phi}{2} \right) \rightarrow 1 + f_\varphi(t, p_\varphi)$  and rewrite Eq. (B.1) as

$$\left( \frac{\partial}{\partial t} - H p_\varphi \frac{\partial}{\partial p_\varphi} \right) F(t, p_\varphi) = \frac{16\pi^2 \Gamma_\phi^{(0)} n_\phi}{m_\phi^2} \delta \left( p_\varphi - \frac{m_\phi}{2} \right), \tag{B.2}$$

with

$$F(t, p_\varphi) \equiv \ln [1 + f_\varphi(t, p_\varphi)]. \tag{B.3}$$

Next, it is straightforward to apply Eq. (B.3) in Ref. [62]. This allows us to obtain  $F$  analytically:

$$\begin{aligned}
F &= \int_{a_I}^a da' \frac{16\pi^2 \Gamma_\phi^{(0)} n_\phi(a')}{m_\phi^2 a' H(a')} \delta \left( p_\varphi \frac{a}{a'} - \frac{m_\phi}{2} \right) \\
&= \int_{a_I}^a da' \frac{16\pi^2 \Gamma_\phi^{(0)} n_\phi(a')}{m_\phi^2 a' H(a')} \frac{a'^2}{a p_\varphi} \delta \left( a' - \frac{2p_\varphi}{m_\phi} a \right) \\
&= \frac{32\pi^2 \Gamma_\phi^{(0)} n_\phi \left( \frac{2p_\varphi}{m_\phi} a \right)}{m_\phi^3 H \left( \frac{2p_\varphi}{m_\phi} a \right)} \Theta \left[ \frac{m_\phi}{2} \frac{a_I}{a} \leq p_\varphi \leq \frac{m_\phi}{2} \right]. \tag{B.4}
\end{aligned}$$

From Eq. (B.4) and Eq. (B.3), we obtain the solution in Eq. (2.18).

## C Phase space integrals for graviton production processes

For  $\varphi\varphi \rightarrow hh$ , the collision term reads

$$\Gamma_h = \frac{1}{2\omega} \int d\Pi_1 d\Pi_2 d\Pi_3 f_1 f_2 \frac{1}{2} \frac{2t^2(s+t)^2}{M_P^4 s^2} (2\pi)^4 \delta^{(4)}(p_1 + p_2 - p_3 - p_4), \tag{C.1}$$

where we have included a symmetry factor of 1/2.

By inserting the following two identities into Eq. (C.1):

$$1 = \int \frac{d^4 q}{(2\pi)^4} (2\pi)^4 \delta^{(4)}(q - p_1 - p_2), \tag{C.2}$$

$$1 = \int \frac{ds}{2\pi} (2\pi) \delta(s + q^2), \tag{C.3}$$

we obtain

$$\begin{aligned}
\Gamma_h &= \frac{1}{4\omega} \int \frac{ds}{2\pi} \int \frac{d^4 q}{(2\pi)^4} \int d\Pi_1 d\Pi_2 f_1 f_2 (2\pi)^4 \delta^{(4)}(p_1 + p_2 - q) \\
&\quad \times \int d\Pi_3 (2\pi)^4 \delta^{(4)}(q - p_3 - p_4) \frac{2t^2(s+t)^2}{M_P^4 s^2} \\
&= \frac{1}{16(2\pi)^2 \omega^2} \int_\omega^\infty dE_q \int_0^{s_{\max 1}} ds \int d\Pi_1 d\Pi_2 f_1 f_2 (2\pi)^4 \delta^{(4)}(p_1 + p_2 - q) \frac{2t^2(s+t)^2}{M_P^4 s^2} \\
&= \frac{1}{64(2\pi)^4 \omega^2} \int_\omega^\infty dE_q \int_0^{E_q} dp_1 f_\varphi(p_1) f_\varphi(E_q - p_1) \\
&\quad \times \int_0^{s_{\max 2}} \frac{ds}{\sqrt{E_q^2 - s}} \int_0^{2\pi} d\varphi \frac{2t^2(s+t)^2}{M_P^4 s^2}, \tag{C.4}
\end{aligned}$$

where  $s_{\max 1} \equiv 4\omega(E_q - \omega)$ ,  $s_{\max 2} \equiv \min[s_{\max 1}, 4E_1(E_q - E_1)]$ , and  $\varphi$  is the azimuthal angle between the planes of  $(\mathbf{q}, \mathbf{p}_1)$  and  $(\mathbf{q}, \mathbf{p}_4)$ .

Next, we use the monochromatic phase-space distribution of  $\varphi$ :

$$f_\varphi(p) = 2\pi^2 \frac{n_\varphi}{p_\varphi^2} \delta(p - p_\varphi), \tag{C.5}$$

where  $p_\varphi = a_I m_\phi / (2a)$  and  $n_\varphi$  scales as  $a^{-3}$ . With the delta function in Eq. (C.5), it is straightforward to proceed with the integration and obtain Eq. (3.9).

For  $\phi \rightarrow \varphi_B \varphi_B h$ , the collision term reads

$$\Gamma_h = \frac{1}{2\omega} \frac{2\mu^2}{M_P^2} \left(1 - \frac{m_\phi}{2\omega}\right)^2 \int d\Pi_1 d\Pi_2 d\Pi_3 f_1 f_2 f_3 (2\pi)^4 \delta^{(4)}(p_1 - p_2 - p_3 - p_4), \quad (\text{C.6})$$

where we have factored the squared matrix element out of the integral.

Since  $f_1$ ,  $f_2$ , and  $f_3$  in the integral are all monochromatic [see Eqs. (A.16) and (C.5)], we integrate out the corresponding delta functions and get

$$\Gamma_h = \frac{1}{2\omega} \frac{2\mu^2}{M_P^2} \left(1 - \frac{m_\phi}{2\omega}\right)^2 \frac{n_\phi n_\varphi^2}{8m_\phi p_\varphi^2} \int \frac{d\Omega_2}{4\pi} \frac{d\Omega_3}{4\pi} (2\pi)^4 \delta(m_\phi - 2p_\varphi - \omega) \delta^{(3)}(p_\varphi \mathbf{n}_2 + p_\varphi \mathbf{n}_3 + \omega \mathbf{n}_4), \quad (\text{C.7})$$

where  $\vec{n}_{2,3,4}$  denote unit vectors of the 2<sup>nd</sup>, 3<sup>rd</sup> and 4<sup>th</sup> particles of the process.

Without loss of generality, we assume that  $\vec{n}_4$  aligns with the  $z$  axis and parameterize  $\vec{n}_{2,3}$  as follows.

$$\vec{n}_i = (s_i \cos \phi_i, s_i \sin \phi_i, c_i) \quad \text{with } i \in \{2, 3\}, \quad (\text{C.8})$$

where  $(s_i, c_i) \equiv (\sin \theta_i, \cos \theta_i)$ .

With the above parameterization, the angular part of the phase space integral can be performed explicitly:

$$\begin{aligned} & \int \frac{d\Omega_2}{4\pi} \frac{d\Omega_3}{4\pi} \delta^{(3)}(p_\varphi \vec{n}_2 + p_\varphi \vec{n}_3 + \omega \vec{n}_4) \\ &= \int \frac{dc_2 d\phi_2}{4\pi} \frac{dc_3 d\phi_2}{4\pi} \frac{1}{p_\varphi^3} \delta\left(\sum_i s_i \cos \phi_i\right) \delta\left(\sum_i s_i \sin \phi_i\right) \delta\left(\frac{\omega}{p_\varphi} + \sum_i c_i\right) = \frac{1}{8\pi p_\varphi^2 \omega}. \end{aligned} \quad (\text{C.9})$$

Therefore, Eq. (C.7) proceeds as follows

$$\begin{aligned} \Gamma_h &= \frac{1}{2\omega} \frac{2\mu^2}{M_P^2} \left(1 - \frac{m_\phi}{2\omega}\right)^2 \frac{n_\phi n_\varphi^2}{8m_\phi p_\varphi^2} (2\pi)^4 \frac{1}{8\pi p_\varphi^2 \omega} \delta(m_\phi - 2p_\varphi - \omega) \\ &= \frac{4\pi^3 \mu^2 n_\varphi^2 n_\phi}{m_\phi^5 M_P^2 \omega^2} \left(1 - \frac{m_\phi}{2\omega}\right)^2 \left(\frac{a}{a_I}\right)^4 \delta(\omega_B - \omega). \end{aligned} \quad (\text{C.10})$$

For  $\phi \rightarrow \varphi_B \varphi h$ , the collision term reads

$$\Gamma_h = \frac{1}{2\omega} \frac{2\mu^2}{M_P^2} \left(1 - \frac{m_\phi}{2\omega}\right)^2 \int d\Pi_1 d\Pi_2 d\Pi_3 f_1 f_2 (2\pi)^4 \delta^{(4)}(p_1 - p_2 - p_3 - p_4), \quad (\text{C.11})$$

similar to Eq. (C.6), but without  $f_3$ . Integrating the delta functions in  $f_1$  and  $f_2$ , we get

$$\Gamma_h = \frac{1}{2\omega} \frac{2\mu^2}{M_P^2} \left(1 - \frac{m_\phi}{2\omega}\right)^2 \frac{n_\phi n_\varphi}{4m_\phi p_\varphi} \int \frac{d\Omega_2}{4\pi} d\Pi_3 (2\pi)^4 \delta^{(4)}(p_1 - p_2 - p_3 - p_4), \quad (\text{C.12})$$

where  $\vec{n}_{2,3,4}$  denote unit vectors of the 2<sup>nd</sup>, 3<sup>rd</sup> and 4<sup>th</sup> particles of the process. Since particle 3 is massless, we have

$$\int d\Pi_3 (2\pi)^4 \delta^{(4)}(p_1 - p_2 - p_3 - p_4) = 2\pi \frac{1}{2E_{124}} \delta(E_{124} - p_{124}), \quad (\text{C.13})$$

where  $E_{124} \equiv |E_1 - E_2 - E_4|$  and  $p_{124} \equiv |\vec{p}_1 - \vec{p}_2 - \vec{p}_4|$ . Next, we perform the angular part of the phase space integral

$$\begin{aligned} & \int \frac{d\Omega_2}{4\pi} d\Pi_3 (2\pi)^4 \delta^{(4)}(p_1 - p_2 - p_3 - p_4) \\ &= \int \frac{d\Omega_2}{4\pi} 2\pi \frac{1}{2E_{124}} \delta(E_{124} - p_{124}) = \frac{\pi}{2E_2 \omega}. \end{aligned} \quad (\text{C.14})$$

Substituting Eq. (C.14) into Eq. (C.12), we obtain

$$\begin{aligned} \Gamma_h &= \frac{1}{2\omega} \frac{2\mu^2}{M_P^2} \left(1 - \frac{m_\phi}{2\omega}\right)^2 \frac{n_\phi n_\varphi}{4m_\phi p_\varphi} \frac{\pi}{2p_\varphi \omega} \\ &= \frac{\pi n_\varphi n_\phi}{2m_\phi^3 \omega^2} \frac{\mu^2}{M_P^2} \left(1 - \frac{m_\phi}{2\omega}\right)^2 \left(\frac{a}{a_I}\right)^2. \end{aligned} \quad (\text{C.15})$$

## References

- [1] R. Allahverdi, R. Brandenberger, F.-Y. Cyr-Racine and A. Mazumdar, *Reheating in Inflationary Cosmology: Theory and Applications*, *Ann. Rev. Nucl. Part. Sci.* **60** (2010) 27 [[1001.2600](#)].
- [2] M.A. Amin, M.P. Hertzberg, D.I. Kaiser and J. Karouby, *Nonperturbative Dynamics Of Reheating After Inflation: A Review*, *Int. J. Mod. Phys. D* **24** (2014) 1530003 [[1410.3808](#)].
- [3] K.D. Lozanov, *Lectures on Reheating after Inflation*, [1907.04402](#).
- [4] B. Barman, N. Bernal and J. Rubio, *Two or three things particle physicists (mis)understand about (pre)heating*, *Nucl. Phys. B* **1018** (2025) 116996 [[2503.19980](#)].
- [5] K. Nakayama and Y. Tang, *Stochastic Gravitational Waves from Particle Origin*, *Phys. Lett. B* **788** (2019) 341 [[1810.04975](#)].
- [6] D. Huang and L. Yin, *Stochastic Gravitational Waves from Inflaton Decays*, *Phys. Rev. D* **100** (2019) 043538 [[1905.08510](#)].
- [7] B. Barman, N. Bernal, Y. Xu and Ó. Zapata, *Gravitational wave from graviton Bremsstrahlung during reheating*, *JCAP* **05** (2023) 019 [[2301.11345](#)].
- [8] B. Barman, N. Bernal, Y. Xu and Ó. Zapata, *Bremsstrahlung-induced gravitational waves in monomial potentials during reheating*, *Phys. Rev. D* **108** (2023) 083524 [[2305.16388](#)].
- [9] S. Kanemura and K. Kaneta, *Gravitational waves from particle decays during reheating*, *Phys. Lett. B* **855** (2024) 138807 [[2310.12023](#)].
- [10] N. Bernal, S. Cléry, Y. Mambrini and Y. Xu, *Probing reheating with graviton bremsstrahlung*, *JCAP* **01** (2024) 065 [[2311.12694](#)].
- [11] A. Tokareva, *Gravitational waves from inflaton decay and bremsstrahlung*, *Phys. Lett. B* **853** (2024) 138695 [[2312.16691](#)].
- [12] W. Hu, K. Nakayama, V. Takhistov and Y. Tang, *Gravitational wave probe of Planck-scale physics after inflation*, *Phys. Lett. B* **856** (2024) 138958 [[2403.13882](#)].
- [13] K.-Y. Choi, E. Lkhagvadorj and S. Mahapatra, *Gravitational wave sourced by decay of massive particle from primordial black hole evaporation*, *JCAP* **07** (2024) 064 [[2403.15269](#)].

[14] B. Barman, N. Bernal, S. Cléry, Y. Mambrini, Y. Xu and Ó. Zapata, *Probing Reheating with Gravitational Waves from Graviton Bremsstrahlung*, in *58<sup>th</sup> Rencontres de Moriond on Electroweak Interactions and Unified Theories*, 5, 2024 [[2405.09620](#)].

[15] R. Inui, Y. Mikura and S. Yokoyama, *Gravitational waves from graviton bremsstrahlung with kination phase*, *Phys. Rev. D* **111** (2025) 043511 [[2408.10786](#)].

[16] Y. Jiang and T. Suyama, *Spectrum of high-frequency gravitational waves from graviton bremsstrahlung by the decay of inflaton: case with polynomial potential*, *JCAP* **02** (2025) 041 [[2410.11175](#)].

[17] D. Das, M. Sanghi and Sourav, *Stochastic gravitational wave from graviton bremsstrahlung in inflaton decay into massive spin 3/2 particles*, [2511.01579](#).

[18] J. Cheng and A. Tokareva, *Weak Gravity Conjecture in the sky: gravitational waves from preheating in Einstein-Maxwell-Scalar EFT*, [2512.10890](#).

[19] Y. Ema, R. Jinno, K. Mukaida and K. Nakayama, *Gravitational Effects on Inflaton Decay*, *JCAP* **05** (2015) 038 [[1502.02475](#)].

[20] Y. Ema, R. Jinno, K. Mukaida and K. Nakayama, *Gravitational particle production in oscillating backgrounds and its cosmological implications*, *Phys. Rev. D* **94** (2016) 063517 [[1604.08898](#)].

[21] Y. Ema, R. Jinno and K. Nakayama, *High-frequency Graviton from Inflaton Oscillation*, *JCAP* **09** (2020) 015 [[2006.09972](#)].

[22] G. Choi, W. Ke and K.A. Olive, *Minimal production of prompt gravitational waves during reheating*, *Phys. Rev. D* **109** (2024) 083516 [[2402.04310](#)].

[23] K. Mudrunka and K. Nakayama, *High Frequency Spectrum of Primordial Gravitational Waves*, [2601.00378](#).

[24] Y. Xu, *Ultra-high frequency gravitational waves from scattering, Bremsstrahlung and decay during reheating*, *JHEP* **10** (2024) 174 [[2407.03256](#)].

[25] N. Bernal, Q.-f. Wu, X.-J. Xu and Y. Xu, *Pre-thermalized gravitational waves*, *JHEP* **08** (2025) 125 [[2503.10756](#)].

[26] X.-J. Xu, Y. Xu, Q. Yin and J. Zhu, *Full-spectrum analysis of gravitational wave production from inflation to reheating*, *JHEP* **10** (2025) 141 [[2505.08868](#)].

[27] N. Bernal and Y. Xu, *Thermal gravitational waves during reheating*, *JHEP* **01** (2025) 137 [[2410.21385](#)].

[28] N. Aggarwal et al., *Challenges and opportunities of gravitational-wave searches at MHz to GHz frequencies*, *Living Rev. Rel.* **24** (2021) 4 [[2011.12414](#)].

[29] N. Aggarwal et al., *Challenges and Opportunities of Gravitational Wave Searches above 10 kHz*, [2501.11723](#).

[30] K. Ichikawa, T. Suyama, T. Takahashi and M. Yamaguchi, *Primordial Curvature Fluctuation and Its Non-Gaussianity in Models with Modulated Reheating*, *Phys. Rev. D* **78** (2008) 063545 [[0807.3988](#)].

[31] M. Drewes, *Measuring the inflaton coupling in the CMB*, *JCAP* **09** (2022) 069 [[1903.09599](#)].

[32] M.A.G. Garcia, K. Kaneta, Y. Mambrini and K.A. Olive, *Inflaton Oscillations and Post-Inflationary Reheating*, *JCAP* **04** (2021) 012 [[2012.10756](#)].

[33] J.F. Dufaux, G.N. Felder, L. Kofman, M. Peloso and D. Podolsky, *Preheating with trilinear interactions: Tachyonic resonance*, *JCAP* **07** (2006) 006 [[hep-ph/0602144](#)].

[34] E.W. Kolb and M.S. Turner, *The Early Universe*, vol. 69 of *Frontiers in Physics*, Addison-Wesley, Redwood City, CA (1990).

[35] PARTICLE DATA GROUP collaboration, *Review of particle physics*, *Phys. Rev. D* **110** (2024) 030001.

[36] C. Caprini and D.G. Figueroa, *Cosmological Backgrounds of Gravitational Waves*, *Class. Quant. Grav.* **35** (2018) 163001 [[1801.04268](#)].

[37] LISA collaboration, *Laser Interferometer Space Antenna*, [1702.00786](#).

[38] M. Punturo et al., *The Einstein Telescope: A third-generation gravitational wave observatory*, *Class. Quant. Grav.* **27** (2010) 194002.

[39] S. Hild et al., *Sensitivity Studies for Third-Generation Gravitational Wave Observatories*, *Class. Quant. Grav.* **28** (2011) 094013 [[1012.0908](#)].

[40] B. Sathyaprakash et al., *Scientific Objectives of Einstein Telescope*, *Class. Quant. Grav.* **29** (2012) 124013 [[1206.0331](#)].

[41] ET collaboration, *Science Case for the Einstein Telescope*, *JCAP* **03** (2020) 050 [[1912.02622](#)].

[42] D. Reitze et al., *Cosmic Explorer: The U.S. Contribution to Gravitational-Wave Astronomy beyond LIGO*, *Bull. Am. Astron. Soc.* **51** (2019) 035 [[1907.04833](#)].

[43] J. Crowder and N.J. Cornish, *Beyond LISA: Exploring future gravitational wave missions*, *Phys. Rev. D* **72** (2005) 083005 [[gr-qc/0506015](#)].

[44] V. Corbin and N.J. Cornish, *Detecting the cosmic gravitational wave background with the big bang observer*, *Class. Quant. Grav.* **23** (2006) 2435 [[gr-qc/0512039](#)].

[45] G.M. Harry, P. Fritschel, D.A. Shaddock, W. Folkner and E.S. Phinney, *Laser interferometry for the big bang observer*, *Class. Quant. Grav.* **23** (2006) 4887.

[46] N. Seto, S. Kawamura and T. Nakamura, *Possibility of direct measurement of the acceleration of the universe using 0.1-Hz band laser interferometer gravitational wave antenna in space*, *Phys. Rev. Lett.* **87** (2001) 221103 [[astro-ph/0108011](#)].

[47] H. Kudoh, A. Taruya, T. Hiramatsu and Y. Himemoto, *Detecting a gravitational-wave background with next-generation space interferometers*, *Phys. Rev. D* **73** (2006) 064006 [[gr-qc/0511145](#)].

[48] PLANCK collaboration, *Planck 2018 results. VI. Cosmological parameters*, *Astron. Astrophys.* **641** (2020) A6 [[1807.06209](#)].

[49] SIMONS OBSERVATORY collaboration, *The Simons Observatory: Science goals and forecasts*, *JCAP* **02** (2019) 056 [[1808.07445](#)].

[50] SIMONS OBSERVATORY collaboration, *The Simons Observatory: Astro2020 Decadal Project Whitepaper*, *Bull. Am. Astron. Soc.* **51** (2019) 147 [[1907.08284](#)].

[51] CMB-S4 collaboration, *CMB-S4 Science Book, First Edition*, [1610.02743](#).

[52] K. Abazajian et al., *CMB-S4 Science Case, Reference Design, and Project Plan*, [1907.04473](#).

[53] CMB-HD collaboration, *Snowmass2021 CMB-HD White Paper*, [2203.05728](#).

- [54] CORE collaboration, *COre (Cosmic Origins Explorer) A White Paper*, [1102.2181](https://arxiv.org/abs/1102.2181).
- [55] EUCLID collaboration, *Euclid Definition Study Report*, [1110.3193](https://arxiv.org/abs/1110.3193).
- [56] I. Ben-Dayan, B. Keating, D. Leon and I. Wolfson, *Constraints on scalar and tensor spectra from  $N_{eff}$* , *JCAP* **06** (2019) 007 [[1903.11843](https://arxiv.org/abs/1903.11843)].
- [57] J. Ghiglieri, J. Schütte-Engel and E. Speranza, *Freezing-in gravitational waves*, *Phys. Rev. D* **109** (2024) 023538 [[2211.16513](https://arxiv.org/abs/2211.16513)].
- [58] M.E. Peskin and D.V. Schroeder, *An Introduction to quantum field theory*, Addison-Wesley, Reading, USA (1995), [10.1201/9780429503559](https://arxiv.org/abs/10.1201/9780429503559).
- [59] S. Weinberg, *Infrared photons and gravitons*, *Phys. Rev.* **140** (1965) B516.
- [60] R. Flauger and S. Weinberg, *Absorption of Gravitational Waves from Distant Sources*, *Phys. Rev. D* **99** (2019) 123030 [[1906.04853](https://arxiv.org/abs/1906.04853)].
- [61] W.-Y. Ai, S.A.R. Ellis and J. Pradler, *Soft Gravitons, Hard Truths: Infrared Safety of Particle Processes in a Gravitational-Wave Background*, [2510.27690](https://arxiv.org/abs/2510.27690).
- [62] Q.-f. Wu and X.-J. Xu, *High-energy and ultra-high-energy neutrinos from Primordial Black Holes*, *JCAP* **02** (2025) 059 [[2409.09468](https://arxiv.org/abs/2409.09468)].